Acta Appl Math (2010) 109: 903–937
DOI 10.1007/s10440-008-9353-9

Classification of Curves in 2D and 3D via Affine Integral Signatures

Shuo Feng · Irina Kogan · Hamid Krim

Received: 20 August 2008 / Accepted: 24 October 2008 / Published online: 7 November 2008

Abstract We propose new robust classification algorithms for planar and spatial curves subjected to affine transformations. Our motivation comes from the problems in computer image recognition. To each planar or spatial curve, we assign a planar signature curve. Curves, equivalent under an affine transformation, have the same signature. The signatures are based on integral invariants, which are significantly less sensitive to small perturbations of curves and noise than classically known differential invariants. Affine invariants are derived in terms of Euclidean invariants. We present two types of signatures: the global and the local signature. Both signatures are independent of curve parameterization. The global signature depends on a choice of the initial point and, therefore, cannot be used for local comparison. The local signature, albeit being slightly more sensitive to noise, is independent of the choice of the initial point and can be used to solve local equivalence problem. An experiment that illustrates robustness of the proposed signatures is presented.

Keywords Euclidean and affine transformations · Equivalence problem for curves · Integral invariants · Signatures · Image recognition

Mathematics Subject Classification (2000) 53A55 · 68T45

I.A. Kogan is supported in part by National Science Foundation (NSF) grant #0728801.
H. Krim is supported in part by Air Force Office of Scientific Research (AFOSR) grant #F49620-98-1-0190.

S. Feng (✉) · H. Krim
ECE Department, North Carolina State University, Raleigh, NC, 27695-7914, USA
e-mail: shuo.feng@intel.com

H. Krim
e-mail: ahk@ncsu.edu

I. Kogan
Department of Mathematics, North Carolina State University, Raleigh, NC, 27695-8205, USA
e-mail: iakogan@ncsu.edu

1 Introduction

In the most general terms the equivalence, or classification, problem for curves, considered in this paper, can be formulated as follows. An action of a group G on $\mathbb{R}^n$ induces an action on the space of curves in $\mathbb{R}^n$. Two curves are called equivalent with respect to this action if there exists an element $g \in G$ that maps one of the curves to the other, or in other words, two curves that belong to the same orbit with respect to the induced action are equivalent. Our motivation comes from the problems in computer vision, since they can be often reduced to a classification problem for curves in $\mathbb{R}^2$ and $\mathbb{R}^3$ with respect to the actions of the Euclidean, affine and projective groups. One can attempt to solve this problem by finding an element g explicitly, or otherwise proving that this element does not exist. This approach has many disadvantages from both theoretical and computational perspectives. More elegant and practical solution to the equivalence problem is obtained by finding sufficient number of quantities that are invariant, or unchanged, under the group action. In the spirit of the Felix Klein Erlangen program (1872), which describes geometry as the study of invariants of group actions on geometric objects, the Euclidean, affine and projective groups are often referred to as geometric groups and the corresponding invariants are called geometric invariants. We note that the Euclidean group is a subgroup of the affine group, whereas the affine group is a subgroup of the projective group.

While geometric invariants have long been used to solve problems in computer vision and image processing [10, 26, 27, 30, 40], designing robust algorithms that are tolerant to noise and image occlusion remains an open problem. Euclidean differential invariants, such as Euclidean curvature and torsion for space curves, are the most classical. The affine and projective counterparts of curvature and torsion are also well known. The dependence of curvature and torsion on high order derivatives (up to order 3 for the Euclidean group, 6 for the affine group and 9 for the projective group), makes numerical approximation of these invariants highly sensitive to noise and, therefore, impractical in computer vision applications. This has motivated a high interest in other types of invariants such as semi-differential, or joint, invariants [4, 29, 37, 38] and various types of integral invariants [17, 23–25, 31]. The term *integral invariants* is used in the literature when an invariant depends on quantities obtained by integration (versus differential invariants that depend on the derivatives). There are various types of integral invariants, and some of them (such as in [31]) are, in fact, mixed: they depend on quantities obtained by integration and on quantities obtained by differentiation. Semi-differential, or joint, invariants are obtained by extending an action to several copies of the same curve, and then computing algebraic and differential invariants on this extended space. This leads to a decrease in the order of derivatives involved in the invariants. The trade-off, however, is the increase in the dimension of the underlying space. Since integration reduces the effect of noise, it is desirable to use purely integral invariants whose computation does not include differentiation.

Although explicit expressions for various types of integral invariants under Euclidean and affine transformations, as well as some other subgroups of the full projective group for curves in $\mathbb{R}^2$ were computed before [17, 23–25, 31], the computational difficulties have thus far prevented the extension to curves in $\mathbb{R}^3$. In [12] a mixed integro-differential affine invariants that only uses first order derivatives along with integrals were computed for curves in $\mathbb{R}^3$. Although improvement over classical differential invariants in classification of curves affected by slight perturbation and noise was achieved, the presence of first order derivatives still affected the performance. In a conference proceedings paper [13], we presented, for the first time, explicit formulae of purely integral Euclidean and affine invariants for spatial curves in $\mathbb{R}^3$. An inductive implementation of the Fels-Olver moving frame construction [11], proposed in [22], was used to simplify the derivation, as it allows one to

construct invariants for the entire group from invariants of its subgroups: in our case, affine invariants in terms of Euclidean ones. In this paper we review the definition and the main steps of derivation of these invariants. In this paper we also introduce two types of signatures based on these invariants: the global and the local integral signature. Two curves related by an affine transformation have the same signature. Both signatures are independent of curve parameterization. The global signature depends on a choice of the initial point and, therefore, cannot be used for local comparison. The local signature, albeit slightly more sensitive to noise, is independent of the choice of the initial point and can be used to solve local equivalence problem, and hence can be applied to curves with occlusions. Although the paper focuses on signatures with respect to the affine group of transformations, the method is easily adapted to a its proper subgroup of Euclidean transformations. We include an experiment that illustrates robustness of the proposed signatures in application to the classification of curves extracted from the images of various surfaces in $\mathbb{R}^3$. Our literature search indicates that this is the first method for classification of *spatial curves* with respect to affine transformations based on purely integral invariants.

The type of integral invariants that we consider is an extension of the invariants introduced by Hann and Hickman [17] for curves in $\mathbb{R}^2$. For planar curves they are obtained by prolonging the action of the group to integrals of the monomials along the curve $\gamma(t) = (x(t), y(t)), t \in [0, 1]$. In other words, integral invariants depend on the initial and current points on the curve, as well as on integral variables $Y^{[i,j]} = \int_0^t X^i Y^j dY$ and $X^{[i,j]} = \int_0^t X^i Y^j dX$, where $X(t) = x(t) - x(0)$ and $Y(t) = y(t) - y(0)$. For example, $I_1(t) = \int_0^t X(t)dY(t) - \frac{1}{2}X(t)Y(t)$ is invariant under the action of the special affine group. Geometrically, I represents the signed area between the curve and the secant (see Fig. 1). In a way, the integral invariants of this type can be thought of as the 1-dimensional analog of moment invariants [8, 34, 41]. The difference, however, lies not only in dimensionality: a moment invariant corresponds a *number* to a surface, whereas an integral invariant corresponds a *curve* to a curve.

Integral invariants depend on parameterization of a curve (or curve sampling in the discrete case). A uniform parameterization is required for two curves to be compared. In order to overcome this limitation, we propose to use signatures. The signature of a curve is obtained by plotting one independent invariant, evaluated on the curve, versus another. Applications of signatures based on differential invariants and on joint invariants to curve classification can be found, for instance, in [1, 4–6, 29]. Signatures based on differential invariants are highly sensitive to noise. Although utilization of joint invariants, decreases noise sensitivity, it does in general increase the dimension of the signature (a joint-invariant signature for a curve might be given by a surface or a higher dimensional manifold, which makes signature comparison challenging). The advantage of *integral signature* proposed here is that it diminishes the effects of noise and does not enlarge dimensionality of the problem. In [24, 25] integral signatures based on integral invariants of different type were

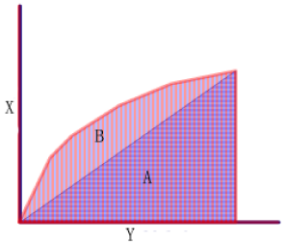

Fig. 1 Invariant $I_1(t) = \int_0^t X(t)dY(t) - \frac{1}{2}X(t)Y(t)$ equals to the area B between the curve and the secant

proposed. This construction is restricted, however, to *planar curves* undergoing Euclidean transformations only.

Several interesting directions of future research emerge from this investigation. From the definition of invariants it follows that equivalent curves have the same signatures. At present, we do not, however, have a general proof of the converse statement, namely that signatures of non-equivalent curves are different (although our experiments support this conjecture). In other words, the separating property of the invariants derived in this paper remains to be established. In the case of differential invariants, the corresponding proof relies on the known structure of differential invariants, established by Tresse [36]—differential invariants form a finitely generated differential algebra. At present, there is no analogous result about the structure of integral invariants, and thus we can only conjecture on the number of separating invariants. The problem of equivalence is closely related to the problem of finding the symmetry group of an object, i.e. the transformations that map the object to itself. Possibility of extracting the symmetry information from the integral signature is another interesting open question. Extension to higher dimensions and other group-actions is also of interest.

Exploring various applications of these invariants to computer image recognition and image processing problems is another important venue of future research. The defining features of 3D or 2D objects are often represented by spatial or planar curves, as illustrated in Fig. 2. Since the images of the object are often taken by the cameras located in various positions and with various focal lengths, the resulting images of the same feature curve are often related by projective transformations, or in many cases by elements of a proper subgroup of the projective group, in particular, by affine and Euclidean transformations [26]. Integral signatures introduced in this paper provide a new tool for establishing equivalence of various images of the same object. In [14] we reported the initial results of applications of Euclidean integral signatures to the problem of face recognition and obtained some promising results. Further investigation in this direction is underway. A thorough comparison of the performance of our method with methods based on other types of constructions, in particular, with methods based on affine invariant Fourier descriptors [3], and affine invariant wavelet representation [35], is planned (see conclusion of the paper for more details). We would like to point out that the vast majority of the existing methods are restricted to the classification problems of planar curves.

The paper is structured as follows. In Sect. 2, after reviewing the basic facts about group actions and invariants, we define the notion of integral jet bundle and integral invariants in a general setting of curves in $\mathbb{R}^n$. Explicit formulae for affine integral invariants in terms of Euclidean ones for curves in $\mathbb{R}^2$ and $\mathbb{R}^3$ are given in Sect. 3, along with their geometric interpretation. The details of their derivation is given in the Appendix. In Sect. 4 we define a global integral signature that classifies curves with a given initial point up to affine transformations. We also define a local signature that is independent of the initial point of a

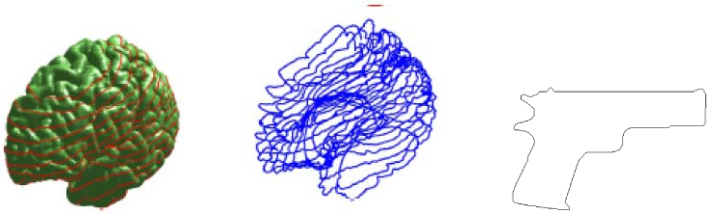

(a) Brain feature curves [28] (b) Gun feature contour

Fig. 2 Examples of feature curves

curve. In Sect. 5 a discrete approximation of the signature construction is tested on curves extracted from 3D objects. The curves are given as discrete sequences of points, with possible additive noise. The experiments show that signature construction gives a robust method for classification of curves under affine transformations. The conclusion section summarizes the results of the paper and indicates the directions of further research.

2 Group Actions and Invariants

In this section we review the basic properties of group actions and invariants, as well as the concept of prolonging the action to jet spaces and the notion of differential invariants. We then introduce the notion of *integral jet space* and define the corresponding prolongation of the action which gives rise to *integral invariants*.

2.1 Definitions

Definition 2.1 An action of a group G on a set S is a map $\alpha\colon G \times S \to S$ that satisfies the following two properties:

1. $\alpha(e, s) = s$, $\forall s \in S$, where e is the identity of the group.
2. $\alpha(g_1, \alpha(g_2, s)) = \alpha(g_1 g_2, s)$, for all $s \in S$ and $g_1, g_2 \in G$.

For $g \in G$ and $s \in S$ we write $\alpha(g, s) = g \cdot s = \overline{s}$.

Definition 2.2 The *orbit* of a point $s \in S$ is the set $O_s = \{g \cdot s | g \in G\}$.

Definition 2.3 A function $f\colon S \to \mathbb{R}$ is called *invariant* if

$$f(g \cdot s) = f(s), \quad \forall g \in G \text{ and } \forall s \in S. \tag{1}$$

Invariant functions are constant along each orbit and can be used to find equivalence classes of objects undergoing various types of transformations.

Let $\mathcal{GL}(n)$ denote a group of non-degenerate $n \times n$ matrices with real entries. Its subgroup of matrices with determinant 1 is denoted by $\mathcal{SL}(n)$. The *orthogonal group* is $\mathcal{O}(n) = \{\mathbf{A} \in \mathcal{GL}(n) | \mathbf{A}\mathbf{A}^T = I\}$, while the *special orthogonal group* is $\mathcal{SO}(n) = \{\mathbf{A} \in \mathcal{O}(n) | \det \mathbf{A} = 1\}$. The semi-direct product of $\mathcal{GL}(n)$ and $\mathbb{R}^n$ is called the *affine group*: $\mathcal{A}(n) = \mathcal{GL}(n) \ltimes \mathbb{R}^n$. Its subgroup $\mathcal{SA}(n) = \mathcal{SL}(n) \ltimes \mathbb{R}^n$ is called the *special affine group*. The *Euclidean group* is $\mathcal{E}(n) = \mathcal{O}(n) \ltimes \mathbb{R}^n$. Its subgroup $\mathcal{SE}(n) = \mathcal{SO}(n) \ltimes \mathbb{R}^n$ is called the *special Euclidean group*.

In the paper we consider the action of the affine group $\mathcal{A}(n)$ and its subgroups on curves $\gamma(t) = (x_1(t), \ldots, x_n(t)), t \in [0, 1]$ in $\mathbb{R}^n$ by a composition of a linear transformation and a translation, for $n = 2$ and $n = 3$:

$$\begin{pmatrix} \overline{x_i(t)} \\ \vdots \\ \overline{x_n(t)} \end{pmatrix} = \mathbf{A} \begin{pmatrix} x_1(t) \\ \vdots \\ x_n(t) \end{pmatrix} + \begin{pmatrix} v_1 \\ \vdots \\ v_n \end{pmatrix}, \tag{2}$$

where the matrix $\mathbf{A} \in \mathcal{GL}(n)$ denotes a linear transformation and the vector $(v_1, \ldots v_n) \in \mathbb{R}^n$ denotes a translation.

2.2 Prolongation of a Group Action

Our goal is to obtain invariants that classify curves up to affine transformations. The classical method of obtaining such invariants is to prolong the action to the set of derivatives $\{x_1^{(k)}, \ldots, x_i^{(k)} | k = 1, \ldots, l\}$ of a sufficiently high order l

$$\overline{x_i^{(1)}}(t) = \frac{d\overline{x_i}(t)}{dt}, \qquad \overline{x_i^{(k+1)}}(t) = \frac{d\overline{x_i^{(k)}}(t)}{dt}. \tag{3}$$

Definition 2.4 Functions of $\{x_1, \ldots, x_n, x_i^{(k)} | i = 1, \ldots, n, k = 1, \ldots, l\}$ that are invariant under the prolonged action (3) are called *differential invariants* of order l.

For the Euclidean action on curves in $\mathbb{R}^3$, the two lowest order invariants are called curvature and torsion, and are classically known in differential geometry. Analogous invariants for the affine and projective groups are also known.

As noted in the introduction, differential invariants are highly sensitive to noise. We introduce integral variables, extending the approach of [17] from planar curves to curves in $\mathbb{R}^n$. Let $\gamma(t)$ be a curve parametrized by $t \in [0, 1]$. We define integral variables

$$x_i^{[\alpha_1, \ldots, \alpha_n]}(t) = \int_0^t x_1(t)^{\alpha_1} \cdots x_n(t)^{\alpha_n} dx_i(t), \quad i = 1, \ldots, n, \tag{4}$$

where the integrals are taken along the curve $\gamma(t)$ and $\alpha_1, \ldots, \alpha_n$ are non-negative integers, such that $\alpha_1 + \cdots + \alpha_{i-1} + \alpha_{i+1} + \cdots + \alpha_n \neq 0$. We call $l = \alpha_1 + \cdots + \alpha_n$ the order of integral variables, and there are totally $n(\frac{(n+l)!}{n!l!} - (l+1))$ of variables of order less than or equal to l. Note that integrals corresponding to $x_i^{[0,\ldots,0,\alpha_i,0,\ldots,0]}(t) = x_i^{\alpha_i+1}(t) - x_i^{\alpha_i+1}(0)$ are not integral variables, according to our definition. Integration-by-parts formula dictates certain relations among the integral variables, the coordinates $x_1(t), \ldots, x_n(t)$ of an arbitrary point on a curve $\gamma(t), t \in [0, 1]$, and the coordinates $x_1^0, \ldots, x_n^0$ of the initial point $\gamma(0)$. For example,

$$\begin{aligned} x_1^{[0,1,0,\ldots,0]}(t) &= \int_0^t x_2(t) dx_1(t) = x_2(t)x_1(t) - x_2^0 x_1^0 - \int_0^t x_1(t) dx_2(t) \\ &= x_2(t)x_1(t) - x_2^0 x_1^0 - x_2^{[1,0,0,\ldots,0]}(t). \end{aligned}$$

It is not difficult to show that there are

$$N_l = (n-1)\frac{(n+l)!}{n!l!} - \sum_{m=1}^{n-1} \frac{(n-m+l)!}{(n-m)!l!}$$

independent integral variables of order less than or equal to l. A canonical choice of such variables is given by:

$$\begin{aligned} x_i^{[\alpha_1, \ldots, \alpha_n]}(t) &= \int_0^t x_1(t)^{\alpha_1} \cdots x_n(t)^{\alpha_n} dx_i(t), \\ &\text{such that } \alpha_1 + \cdots + \alpha_{i-1} > 0, \ i = 1, \ldots, n. \end{aligned} \tag{5}$$

In other words, there is a non-zero entry in the first $i-1$ components of the tuple $[\alpha_1, \ldots, \alpha_n]$. For example, variable $x_2^{[1,0,0,\ldots,0]}$ is canonical, but $x_2^{[0,0,1,0,\ldots,0]}$ and $x_1^{[1,1,0,\ldots,0]}$ are not canonical.

Definition 2.5 Let $\mathcal{I}^l$ be an N_l-dimensional space of independent integral variables of order l and less, then the *integral jet space of order l* (denoted $\mathcal{S}^l$) is defined to be a direct product of $\mathcal{I}^l$ and two copies of $\mathbb{R}^n$, i.e. $\mathcal{S}^l = \mathcal{I}^l \times \mathbb{R}^n \times \mathbb{R}^n$. The coordinates $x_1, \ldots, x_n$ of the first copy of $\mathbb{R}^n$ represent an arbitrary point on a curve $\gamma(t), t \in [0, 1]$, and coordinates $x_1^0, \ldots, x_n^0$ of the second copy of $\mathbb{R}^n$ represent the initial point $\gamma(0)$.

The action (2) can be prolonged to the curves on the jet space as follows:

$$\begin{gathered}
\begin{pmatrix} \overline{x_i}(t) \\ \vdots \\ \overline{x_n}(t) \end{pmatrix} = \mathbf{A} \begin{pmatrix} x_1(t) \\ \vdots \\ x_n(t) \end{pmatrix} + \begin{pmatrix} v_1 \\ \vdots \\ v_n \end{pmatrix}, \\
\begin{pmatrix} \overline{x_i^0} \\ \vdots \\ \overline{x_n^0} \end{pmatrix} = \mathbf{A} \begin{pmatrix} x_1^0 \\ \vdots \\ x_n^0 \end{pmatrix} + \begin{pmatrix} v_1 \\ \vdots \\ v_n \end{pmatrix}, \\
\overline{x_i^{[\alpha_1,\ldots,\alpha_n]}}(t) = \int_0^t \overline{x_1}^{\alpha_1}(t) \cdots \overline{x_n}^{\alpha_n}(t) d\overline{x_i}(t).
\end{gathered} \tag{6}$$

It is important that the integration-by-parts relations among the integral variables are respected by the prolonged action, and therefore the action on the integral jet space $\mathcal{S}^l$ is well defined.

Definition 2.6 A function on $\mathcal{S}^l$ which is *invariant* under the prolonged action (6) is called *integral invariant of order l*.

By introducing new variables

$$X_i(t) = x_i(t) - x_i^0, \quad i = 1, \ldots, n \tag{7}$$

and making the corresponding substitution into the integrals, we reduce the problem of finding invariants under the action (6) to an equivalent but simpler problem of finding invariant functions of variables $\{X_1, \ldots, X_n, X_i^{[\alpha_1,\ldots,\alpha_n]} | i = 1 \ldots n\}$ under the action of $GL(n)$ defined by

$$\begin{gathered}
\begin{pmatrix} \overline{X_i}(t) \\ \vdots \\ \overline{X_n}(t) \end{pmatrix} = \mathbf{A} \begin{pmatrix} X_1(t) \\ \vdots \\ X_n(t) \end{pmatrix}, \\
\overline{X_i^{[\alpha_1,\ldots,\alpha_n]}}(t) = \int_0^t \overline{X_1}^{\alpha_1}(t) \cdots \overline{X_n}^{\alpha_n}(t) d\overline{X_i}(t).
\end{gathered} \tag{8}$$

Invariants with respect to (6) may be obtained from invariants with respect to (8) by making substitution (7).[1] Invariants with respect to a very general class of actions of con-

[1] This reduction by the group of translations can be put in the context of inductive method described in Appendix. We feel, however, that making this step "upfront" makes the presentation more transparent.

tinuous finite-dimensional groups on manifolds can be computed using Fels-Olver generalization [11] of Cartan's moving frame method (see also its algebraic reformulation [19]). The method consists of choosing a cross-section to the orbits and finding the coordinates of the projection along the orbits of a generic point on a manifold to the cross-section (see Appendix for more details). It can be, in theory, applied to find the invariants under the action described by (8) for arbitrary n. Hann and Hickman [17] used Fels-Olver method to compute integral invariants for *planar curves* ($n = 2$) under affine transformations and a certain subgroup of projective transformations. The corresponding derivation of invariants for *spatial curves* ($n = 3$) remained, however, out of reach due to computational complexity (it is often the case in the computational invariant theory that practical computations become unfeasible as the dimension of the group increases, despite the availability of a theoretical method to compute them [9, 33]). In [13], we derived, for the first time, integral invariants under the Euclidean and affine transformations for *spatial curves* using an inductive variation of the moving frame method [22], which allows one to construct invariants for the entire group in terms of invariants of its subgroups: in our case, affine invariants in terms of Euclidean. Explicit derivation of invariants for curves in the spaces of higher dimension ($n > 3$) remains an open problem, which seems at present, to be of more theoretical, rather than of practical interest.

3 Integral Invariants for Planar and Spatial Curves

In this section we present explicit expressions for integral invariants for $n = 2$ (planar curves) and $n = 3$ (spatial curves) under the affine action (6). The affine invariants are written in terms of the Euclidean invariants. We discuss their properties and geometric interpretation. The inductive derivation of these invariants is outlined in the Appendix.

3.1 Integral Affine Invariants for Curves in $\mathbb{R}^2$

We prolong the standard affine group action on curves in $\mathbb{R}^2$:

$$\begin{pmatrix} \overline{x}(t) \\ \overline{y}(t) \end{pmatrix} = \begin{pmatrix} a_{11} & a_{12} \\ a_{21} & a_{22} \end{pmatrix} \begin{pmatrix} x(t) \\ y(t) \end{pmatrix} + \begin{pmatrix} v_1 \\ v_2 \end{pmatrix}, \qquad \det \begin{pmatrix} a_{11} & a_{12} \\ a_{21} & a_{22} \end{pmatrix} \neq 0,$$

to integral variables up to the third order.

By translating the initial point $\gamma(0)$ to the origin and making the corresponding substitution $X(t) = x(t) - x(0), Y(t) = y(t) - y(0)$ in the integrals, we reduce the problem to computing invariants under the action (8) with $n = 2$. Among 12 integral variables

$$\begin{aligned} X^{[i,j]}(t) &= \int_0^t X(t)^i Y(t)^j dX(t), \quad j \neq 0, i + j \leq 3, \\ Y^{[i,j]}(t) &= \int_0^t X(t)^i Y(t)^j dY(t), \quad i \neq 0, i + j \leq 3 \end{aligned} \tag{9}$$

we make a canonical choice of 6 independent: $Y^{[1,0]}, Y^{[2,0]}, Y^{[1,1]}, Y^{[3,0]}, Y^{[2,1]}, Y^{[1,2]}$, as suggested by formula (5). The rest can be expressed in terms of the canonical variables using integration-by-parts formulas, as follows:

$$\begin{aligned} X^{[0,1]} &= XY - Y^{[1,0]}, \\ X^{[0,2]} &= XY^2 - 2Y^{[1,1]}, \end{aligned}$$

$$
\begin{aligned}
X^{[1,1]} &= \frac{1}{2}X^2Y - \frac{1}{2}Y^{[2,0]},\\
X^{[1,2]} &= \frac{1}{2}X^2Y^2 - Y^{[2,1]},\\
X^{[0,3]} &= Y^3X - 3Y^{[1,2]},\\
X^{[2,1]} &= \frac{1}{3}X^3Y - \frac{1}{3}Y^{[3,0]}.
\end{aligned}
\tag{10}
$$

This reduces the problem to finding invariants under the following $GL(2)$-action on $\mathbb{R}^8$, where $\det \mathbf{A} := a_{11}a_{22} - a_{21}a_{21}$

$$
\begin{aligned}
\overline{X} &= a_{11}X + a_{12}Y, \qquad \overline{Y} = a_{21}X + a_{22}Y,\\
\overline{Y^{[1,0]}} &= (\det \mathbf{A})Y^{[1,0]} + \frac{1}{2}a_{11}a_{21}X^2 + a_{12}a_{21}XY + \frac{1}{2}a_{12}a_{22}Y^2,\\
\overline{Y^{[1,1]}} &= (\det \mathbf{A})\left(a_{22}Y^{[1,1]} + \frac{1}{2}a_{21}Y^{[2,0]}\right) + \frac{1}{3}{a_{21}}^2a_{11}X^3\\
&\quad + \frac{1}{2}a_{21}(a_{11}a_{22} + a_{12}a_{21})X^2Y + a_{21}a_{12}a_{22}XY^2 + \frac{1}{3}{a_{22}}^2a_{12}Y^3,\\
\overline{Y^{[2,0]}} &= (\det \mathbf{A})\left(a_{11}Y^{[2,0]} + 2a_{12}Y^{[1,1]}\right) + \frac{1}{3}a_{11}^2a_{21}X^3\\
&\quad + a_{11}a_{12}a_{21}X^2Y + a_{12}^2a_{21}XY^2 + \frac{1}{3}a_{11}a_{12}a_{21}Y^3,\\
\overline{Y^{[1,2]}} &= (\det \mathbf{A})\left(a_{22}^2Y^{[1,2]} + \frac{1}{3}a_{21}^2Y^{[3,0]} + a_{21}a_{22}Y^{[2,1]}\right)\\
&\quad + \frac{1}{4}a_{11}{a_{21}}^3X^4 + \frac{1}{3}a_{21}^2(2a_{11}a_{22} + a_{12}a_{21})X^3Y\\
&\quad + \frac{1}{2}a_{21}a_{22}(2a_{12}a_{21} + a_{11}a_{22})X^2Y^2 + a_{12}a_{21}{a_{22}}^2XY^3 + \frac{1}{4}a_{12}{a_{22}}^3Y^4,\\
\overline{Y^{[2,1]}} &= (\det \mathbf{A})\left((a_{11}a_{22} + a_{12}a_{21})Y^{[2,1]} + 2a_{12}a_{22}Y^{[1,2]} + \frac{2}{3}a_{11}a_{21}Y^{[3,0]}\right)\\
&\quad + \frac{1}{4}a_{11}^2a_{21}^2X^4 + \frac{1}{3}a_{11}a_{21}(a_{11}a_{22} + 2a_{12}a_{21})X^3Y\\
&\quad + \frac{1}{2}a_{12}a_{21}(2a_{11}a_{22} + a_{12}a_{21})X^2Y^2 + a_{12}^2a_{21}a_{22}XY^3 + \frac{1}{4}{a_{12}}^2{a_{22}}^2Y^4,\\
\overline{Y^{[3,0]}} &= (\det \mathbf{A})\left(a_{11}^2Y^{[3,0]} + 3a_{12}^2Y^{[1,2]} + 3a_{11}a_{12}Y^{[2,1]}\right) + \frac{1}{4}a_{11}^3a_{21}X^4\\
&\quad + a_{11}^2a_{12}a_{21}X^3Y + \frac{3}{2}a_{11}a_{12}^2a_{21}X^2Y^2 + a_{12}^3a_{21}Y^3X + \frac{1}{4}a_{12}^3a_{22}Y^4.
\end{aligned}
\tag{11}
$$

We restrict the above action to the subgroup $\mathcal{S}O(2)$ of rotation matrices by setting $a_{11} = \cos\phi, a_{12} = -\sin\phi, a_{21} = \sin\phi, a_{22} = \cos\phi$. We use the moving frame method to find invariants as described in the Appendix. Computationally this reduces to the substitution $a_{11} = \frac{X}{r}, a_{12} = \frac{Y}{r}, a_{21} = \frac{-Y}{r}, a_{22} = \frac{X}{r}$, where $r = \sqrt{X^2 + Y^2}$ in (11). The resulting

non-constant expressions comprise a set of generating invariants for the $SO(2)$ action:

$$
\begin{aligned}
X_{SE} &= \sqrt{X^2+Y^2} = r,\\
Y^{[1,0]}_{SE} &= Y^{[1,0]} - \frac{XY}{2},\\
Y^{[1,1]}_{SE} &= \frac{1}{r}\left(Y^{[1,1]}X - \frac{1}{2}Y^{[2,0]}Y - \frac{1}{6}X^2Y^2\right),\\
Y^{[2,0]}_{SE} &= \frac{1}{r}\left(Y^{[2,0]}X + 2Y^{[1,1]}Y - \frac{1}{3}X^3Y - \frac{2}{3}XY^3\right),\\
Y^{[1,2]}_{SE} &= \frac{1}{r^2}\left(Y^{[1,2]}X^2 - Y^{[2,1]}XY + \frac{1}{3}Y^{[3,0]}Y^2 - \frac{1}{12}X^3Y^3\right),\\
Y^{[2,1]}_{SE} &= \frac{1}{r^2}\left(Y^{[2,1]}(X^2-Y^2) + 2Y^{[1,2]}XY + \frac{2}{3}Y^{[3,0]}XY - \frac{1}{4}X^2Y^4 - \frac{1}{12}X^4Y^2\right),\\
Y^{[3,0]}_{SE} &= \frac{1}{r^2}\left(Y^{[3,0]}X^2 + 3Y^{[1,2]}Y^2 + 3Y^{[2,1]}XY - \frac{1}{4}X^5Y - \frac{3}{4}X^3Y^3 - \frac{3}{4}XY^5\right).
\end{aligned}
\tag{12}
$$

The invariants with respect to the special Euclidean group are obtained by making a substitution of $Y = y - y^0$ and $X = x - x^0$ in the above expressions (12):[2] We note that since r is invariant, the expressions in the parenthesis in the above formulas are also invariant.

We use the inductive approach, described in the Appendix, to build invariants under the $SL(2)$-action defined by (11) with the condition $\det \mathbf{A} = 1$. The inductive method yields $\mathcal{SA}(2)$-invariants in terms of $\mathcal{SE}(2)$-invariants (12):

$$
\begin{aligned}
Y^{[1,0]}_{SA} &= Y^{[1,0]}_{SE} = Y^{[1,0]} - \frac{XY}{2},\\
Y^{[1,1]}_{SA} &= X_{SE}Y^{[1,1]}_{SE} = Y^{[1,1]}X - \frac{1}{2}Y^{[2,0]}Y - \frac{1}{6}X^2Y^2,\\
Y^{[1,2]}_{SA} &= Y^{[1,2]}_{SE}X^2_{SE} = Y^{[1,2]}X^2 - Y^{[2,1]}XY + \frac{1}{3}Y^{[3,0]}Y^2 - \frac{1}{12}X^3Y^3,\\
Y^{[2,1]}_{SA} &= Y^{[2,1]}_{SE} - \frac{Y^{[2,0]}_{SE}}{Y^{[1,1]}_{SE}}Y^{[1,2]}_{SE},\\
Y^{[3,1]}_{SA} &= \frac{1}{X^2_{SE}}\left(Y^{[3,0]}_{SE} + \frac{3}{2}\frac{Y^{[2,0]}_{SE}}{Y^{[1,1]}_{SE}}Y^{[2,1]}_{SE} + \frac{3}{4}\left(\frac{Y^{[2,0]}_{SE}}{Y^{[1,1]}_{SE}}\right)^2 Y^{[1,2]}_{SE}\right).
\end{aligned}
\tag{13}
$$

By replacing (X, Y) with $(x - x^0, y - y^0)$ in (13) we return to the integral jet space coordinates. In particular, $Y^{[1,0]}_{SA} = Y^{[1,0]} - \frac{1}{2}XY = \int_0^t (x - x^0)dy - \frac{1}{2}(x - x^0)(y - y^0)$.

The following three special affine invariants are used in the next section to solve the classification problem with respect to both special and full affine groups:

[2]The notation for invariants suggests a certain correspondence between the invariants and the coordinate functions of the integral jet space, which we make clear in the Appendix.

$$
\begin{aligned}
I_1 &= Y_{\mathcal{SA}}^{[1,0]} = Y^{[1,0]} - \frac{1}{2}XY,\\
I_2 &= Y_{\mathcal{SA}}^{[1,1]} = Y^{[1,1]}X - \frac{1}{2}Y^{[2,0]}Y - \frac{1}{6}X^2Y^2,\\
I_3 &= Y_{\mathcal{SA}}^{[1,2]} = Y^{[1,2]}X^2 - Y^{[2,1]}XY + \frac{1}{3}Y^{[3,0]}Y^2 - \frac{1}{12}X^3Y^3.
\end{aligned}
\tag{14}
$$

To obtain invariants with respect to the full affine group we need to consider the effect of reflections and arbitrary scaling on the above invariants. We note that the transformation $x \to \lambda x$ and $y \to -\lambda y$ induces the transformation $I_1 \to -\lambda^2 I_1$, $I_2 \to \lambda^4 I_2$ and $I_3 \to -\lambda^6 I_3$. The following rational expressions are thus invariant with respect to the full affine group:

$$
\begin{aligned}
I_2^{\mathcal{A}} &= \frac{I_2}{I_1^2} = \frac{Y^{[1,1]}X - \frac{1}{2}Y^{[2,0]}Y - \frac{1}{6}X^2Y^2}{(Y^{[1,0]} - \frac{1}{2}XY)^2},\\
I_3^{\mathcal{A}} &= \frac{I_3}{I_1^3} = \frac{Y^{[1,2]}X^2 - Y^{[2,1]}XY + \frac{1}{3}Y^{[3,0]}Y^2 - \frac{1}{12}X^3Y^3}{(Y^{[1,0]} - \frac{1}{2}XY)^3}.
\end{aligned}
\tag{15}
$$

The first of the above invariants is equivalent to the one obtained in [17].

3.2 Geometric Interpretation of Invariants for Planar Curves

The first two integral invariants (14) readily lend themselves to a geometric interpretation. Invariants I_1 is the signed area B between the curve segment and the secant (see Fig. 1 in the Introduction). Indeed, the term $Y^{[1,0]}$ in the invariant I_1 is the signed area between the curve $\gamma(t)$ (whose initial point is translated to the origin) and the Y-axis, while $\frac{XY}{2}$ is the signed area of the triangle A. Their difference is the area B. Since the $\mathcal{SA}(2)$-action preserves areas, I_1 is clearly an invariant.

The interpretation of I_2 is slightly more subtle. Using that $Y^{[2,0]} = X^2Y - 2X^{[1,1]}$ and rearranging the terms we rewrite I_2 as idea), and (16) is rewritten as

$$
\begin{aligned}
I_2 &= -\frac{1}{3}((X^2Y^2 - 3XY^{[1,1]}) + (X^2Y^2 - 3YX^{[1,1]})),\\
&\text{where } X = x - x^0,\ Y = y - y^0.
\end{aligned}
\tag{16}
$$

Further, the curve $\gamma(t)$ is lifted from $\mathbb{R}^2$ to $\mathbb{R}^3$ by defining $z(t) = x(t)y(t)$ (similarly to the kernel idea), and (16) is rewritten as

$$
\begin{aligned}
I_2 &= -\frac{1}{3}\left(\left(XYZ - 3X\int_0^t ZdY\right) + \left(XYZ - 3Y\int_0^t ZdX\right)\right),\\
&\text{where } Z = XY = (x - x^0)(y - y^0).
\end{aligned}
\tag{17}
$$

The geometric meaning of $(XYZ - 3X\int_0^t ZdY)$ is illustrated in Fig. 3. The term $\int_0^t ZdY$ is the signed area "under" the plane curve $(Y(t), Z(t))$ in the YZ-plane. Thus $X\int_0^t ZdY$ is the signed volume C under the surface $F = \gamma(t) \times [0, X(t)]$ in Fig. 3. Since XYZ is the signed volume of a rectangular prism ($C + D$ in Fig. 3), then $XYZ - 3X\int_0^t ZdY$ is the signed volume of the rectangular prism ($C + D$) minus three times the volume C "under" the surface $\gamma(t) \times [0, X(t)]$. Interchanging X and Y we obtain a similar interpretation for $XYZ - 3Y\int_0^t ZdX$.

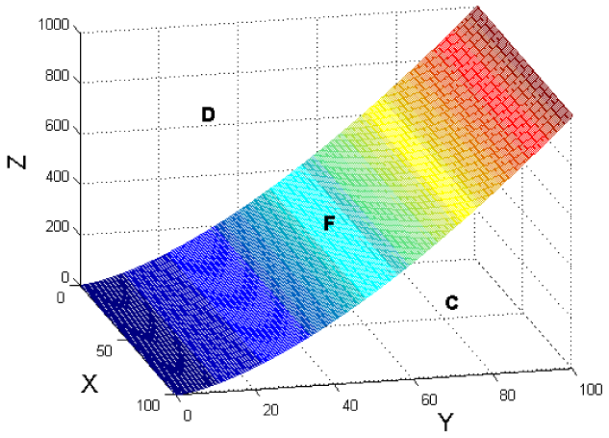

Fig. 3 Geometric interpretation of the invariants I_2

3.3 Integral Affine Invariants for Curves in $\mathbb{R}^3$

We prolong the standard affine group action on curves in $\mathbb{R}^3$:

$$\begin{pmatrix}\overline{x}(t)\\ \overline{y}(t)\\ \overline{z}(t)\end{pmatrix}=\begin{pmatrix}a_{11} & a_{12} & a_{13}\\ a_{21} & a_{22} & a_{23}\\ a_{31} & a_{32} & a_{33}\end{pmatrix}\begin{pmatrix}x(t)\\ y(t)\\ z(t)\end{pmatrix}+\begin{pmatrix}v_1\\ v_2\\ v_3\end{pmatrix},\qquad \det\begin{pmatrix}a_{11} & a_{12} & a_{13}\\ a_{21} & a_{22} & a_{23}\\ a_{31} & a_{32} & a_{33}\end{pmatrix}\neq 0,$$

to integral variables up to second order. We translate the initial point $\gamma(0)$ to the origin, and make the corresponding substitution $X(t)=x(t)-x(0), Y(t)=y(t)-y(0), Z(t)=z(t)-z(0)$ in the integrals. This reduces the problem to computing $SL(3)$-invariants under the action (8) with $n=3$. Among 21 integral variables

$$\begin{aligned}X^{[i,j,k]}(t)&=\int_0^t X(t)^i Y(t)^j Z(t)^k dX(t),\quad j+k\neq 0, i+j+k\leq 2,\\ Y^{[i,j,k]}(t)&=\int_0^t X(t)^i Y(t)^j Z(t)^k dY(t),\quad i+k\neq 0, i+j+k\leq 2,\\ Z^{[i,j,k]}(t)&=\int_0^t X(t)^i Y(t)^j Z(t)^k dZ(t),\quad i+j\neq 0, i+j+k\leq 2,\end{aligned}\tag{18}$$

we choose 11 independent:[3] $X^{[1,1,0]}$, $X^{[1,0,1]}$, $X^{[0,2,0]}$, $Z^{[1,0,0]}$, $Y^{[1,0,0]}$, $Y^{[1,0,1]}$, $Z^{[0,1,0]}$, $Z^{[0,1,1]}$, $Z^{[0,2,0]}$, $Z^{[1,0,1]}$, $Z^{[1,1,0]}$. The rest can be expressed in terms of those using the integration-by-parts formula. Using the inductive approach, we first compute the invariants with respect to rotations $SO(3)$. We find the following 8 independent invariants. (See Appendix for details of the derivation.) $SE(3)$-invariants are obtained by replacing (X, Y, Z) with $(x-x^0, y-y^0, z-z^0)$. Let $R=\sqrt{X^2+Y^2+Z^2}$ and $\Upsilon=\sqrt{(Z_R^{[0,2,0]})^2+4(Z_R^{[0,1,1]})^2}$

[3]The canonical choice dictated by (5) is $Y^{[1,0,0]}$, $Y^{[2,0,0]}$, $Y^{[1,1,0]}$, $Y^{[1,0,1]}$, $Z^{[1,0,0]}$, $Z^{[0,1,0]}$, $Z^{[0,1,1]}$, $Z^{[0,2,0]}$, $Z^{[2,0,0]}$, $Z^{[1,0,1]}$, $Z^{[1,1,0]}$. We made a computation with an equivalent but non-canonical set of variables.

then

$$
\begin{aligned}
X_{SE} &= R \\
Z_{SE}^{[0,1,0]} &= \frac{1}{R}(XYZ - 2XZ^{[0,1,0]} + 2YZ^{[1,0,0]} - 2ZY^{[1,0,0]}), \\
Y_{SE}^{[1,0,0]} &= \frac{1}{\Upsilon}(Z_R^{[0,2,0]} Y_R^{[1,0,0]} + 2Z_R^{[0,1,1]} Z_R^{[1,0,0]}), \\
Y_{SE}^{[1,0,1]} &= \frac{1}{\Upsilon^2}(2Z_R^{[0,2,0]} Z_R^{[0,1,1]} Z_R^{[1,0,1]} + Z_R^{[0,1,1]} Z_R^{[0,2,0]} X_R^{[0,2,0]} \\
&\quad - 4Z_R^{[0,1,1]^2} Z_R^{[1,1,0]} + Z_R^{[0,2,0]^2} Y_R^{[1,0,1]}), \\
Z_{SE}^{[0,2,0]} &= \Upsilon, \\
Z_{SE}^{[1,0,1]} &= \frac{1}{\Upsilon^2}(Z_R^{[0,2,0]^2} Z_R^{[1,0,1]} - 2Z_R^{[0,2,0]} Z_R^{[0,1,1]} Z_R^{[1,1,0]} - 2Z_R^{[0,1,1]^2} X_R^{[0,2,0]} \\
&\quad - 2Z_R^{[0,1,1]} Z_R^{[0,2,0]} Y_R^{[1,0,1]}), \\
Z_{SE}^{[1,1,0]} &= \frac{1}{\Upsilon^2}(2Z_R^{[0,2,0]} Z_R^{[0,1,1]} Z_R^{[1,0,1]} + Z_R^{[0,1,1]} Z_R^{[0,2,0]} X_R^{[0,2,0]} \\
&\quad - 4Z_R^{[0,1,1]^2} Y_R^{[1,0,1]} + Z_R^{[0,2,0]^2} Z_R^{[1,1,0]}),
\end{aligned}
\tag{19}
$$

where expressions $Z_R^{[1,0,0]}$, $Z_R^{[0,1,0]}$, $Y_R^{[1,0,0]}$, $Z_R^{[0,1,1]}$, $Z_R^{[0,2,0]}$, $Z_R^{[1,0,1]}$, $Z_R^{[1,1,0]}$, $Y_R^{[1,0,1]}$, $X_R^{[1,1,0]}$, $X_R^{[1,0,1]}$, $X_R^{[0,2,0]}$ are provided at the end of the Appendix. Note that since R and Υ are invariant, then so are all expression in the parenthesis of (19).

Using the inductive approach, we obtain the expressions for $SA(3)$-invariants in terms of $SE(3)$-invariants.

$$
\begin{aligned}
X_{SA} &= Z_{SE}^{[0,1,0]} X_{SE}, \\
Y_{SA}^{[1,0,1]} &= \frac{2Y_{SE}^{[1,0,1]} Z_{SE}^{[0,1,0]} - 2Z_{SE}^{[0,1,0]} Z_{SE}^{[1,1,0]} + 3Z_{SE}^{[0,2,0]} Z_{SE}^{[1,0,0]}}{2Z_{SE}^{[0,1,0]}} - \frac{1}{2}, \\
Z_{SA}^{[1,0,1]} &= \frac{Z_{SE}^{[1,0,1]} Z_{SE}^{[0,2,0]^2}}{Z_{SE}^{[0,1,0]^3}}.
\end{aligned}
\tag{20}
$$

We introduce a simpler notation for the special affine invariants which will subsequently be used to solve the classification problem with respect to both the special and the full affine groups:

$$
\begin{aligned}
J_1 &= X_{SA} = n_1 X + n_2 Z - n_3 Y, \\
J_2 &= -4\left(Y_{SA}^{[1,0,1]} + \frac{1}{2}\right) X_{SA} \\
&= 2n_2(XYZ^2 - 3Z^{[0,1,1]} X + 3YZ^{[1,0,1]} - ZZ^{[1,1,0]} - 2ZY^{[1,0,1]}) \\
&\quad + n_3(2XY^2 Z + 3XZ^{[0,2,0]} - 3ZX^{[0,2,0]} - 4YZ^{[1,1,0]} - 2YY^{[1,0,1]}) \\
&\quad - 2n_1(3YX^{[1,0,1]} - 3ZX^{[1,1,0]} + XZ^{[1,1,0]} - XY^{[1,0,1]}), \\
J_3 &= \frac{27}{8} Z_{SA}^{[1,0,1]} X_{SA}^3,
\end{aligned}
\tag{21}
$$

where $X = x - x^0$, $Y = y - y^0$, $Z = z - z^0$ and $n_1 = \frac{YZ}{2} - Z^{[0,1,0]}$, $n_2 = \frac{XY}{2} - Y^{[1,0,0]}$, $n_3 = \frac{XZ}{2} - Z^{[1,0,0]}$. The expression of the third invariant in terms of the original integral variables is too long to be included.

To obtain the invariants with respect to the full affine group we consider the effect of reflection and scaling on these invariants. For $\lambda \in \mathbb{R}$ scaling $(x, y, z) \to (\lambda x, \lambda y, -\lambda z)$ induces scaling $J_1 \to -\lambda^3 J_1$, $J_2 \to \lambda^6 J_2$ and $J_3 \to \lambda^6 J_3$. We therefore obtain the following two invariants with respect to the full affine group of transformations:

$$J_2^{\mathcal{A}} = \frac{J_2}{J_1^2} \quad \text{and} \quad J_3^{\mathcal{A}} = \frac{J_3}{J_1^2}. \tag{22}$$

3.4 Geometric Interpretation of Invariants for Spatial Curves

The first invariant J_1 may be viewed as an extension of the 2D invariant I_1 to 3D. Indeed, n_1, n_2, and n_3 represent exactly the same area as the 2D invariant I_1 (in Fig. 3) in three coordinate planes. They are extended to a volume of a three-dimensional solid, by multiplying by X, Z, and Y respectively. For example, $n_1 X$ is the volume C under surface F in Fig. 3, and $n_2 Z$ and $n_3 Y$ are similar volumes obtained by relabelling of X, Y, Z axis. Therefore, the invariant J_1 is the summation of two volumes $n_1 X$ and $n_2 Z$ minus the volume $n_3 Y$. The geometric interpretation of the invariants J_2 and J_3, however, remains at the present time unclear to us.

4 Curve Classification via Integral Signatures

The integral invariants derived in the previous section depend on the choice of the initial point and the parameterization of a curve. For instance, consider a planar curve $\gamma(t) = (1/2 \sin t - \cos t + 1, \sin^2 t + \cos t - 1)$, shown in Fig. 4a. A curve $\overline{\gamma}(t)$ (Fig. 4b) is obtained from $\gamma(t)$ by a special affine transformation $\left(\begin{smallmatrix} 2 & 1 \\ 2 & 1.5 \end{smallmatrix}\right)$. A curve $\overline{\gamma_a(t)}$ (Fig. 4c) is obtained from $\gamma(t)$ by a full affine transformation $\left(\begin{smallmatrix} 2 & 2 \\ 4 & 3 \end{smallmatrix}\right)$.

The integral invariants I_1 and I_2 for curves in Fig. 4a and b with a matching parameterization coincide and are shown in Fig. 5a and b.

As illustrated in Fig. 5c and d, these invariants change under reparametrization $\tau = \sqrt{t+1}$. Therefore the graph of invariants with respect to an arbitrary parameter can not be used for curves comparison. In theory one can achieve a uniform affine invariant curve parameterization by using an affine analog of the Euclidean arc-length parameter $d\alpha = \kappa^{1/3} ds$, where κ is Euclidean curvature and ds is Euclidean arc-length. We would like, however, to keep our methods derivative free. Even when the uniform parameterization is achieved, the dependence of the invariants on the choice of the initial point presents another comparison challenge for matching closed curves, or for matching parts of the contours.

The signature construction, proposed in this section, leads to classification methods which are independent of parametrization and of the initial point. Inspired by signatures based on differential invariants [6], we use integral invariants to construct two types of signatures that classify curves under affine transformation: the global signature and the local signature. *Global integral signature* is independent of parametrization, but *is dependent* on the choice of the initial point and can not be used to compare partial contours. *Local integral signature* is independent of both the initial point and parametrization. They can be used to compare parts of contours and can therefore be used on images with occlusions. As our experiments illustrate they are slightly more sensitive to noise than global signatures, but still provide robust classification results.

Fig. 4 Planar curve γ and its transformations

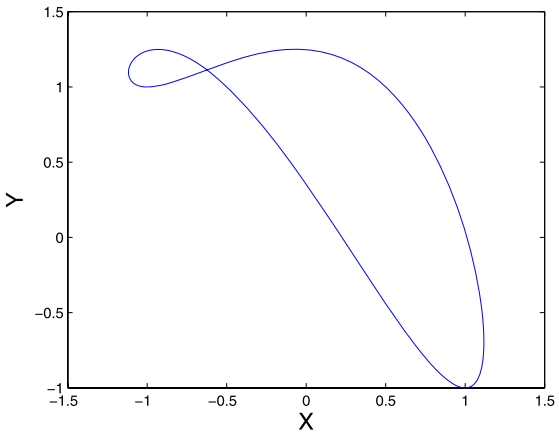

(a) Curve $\gamma(t)$

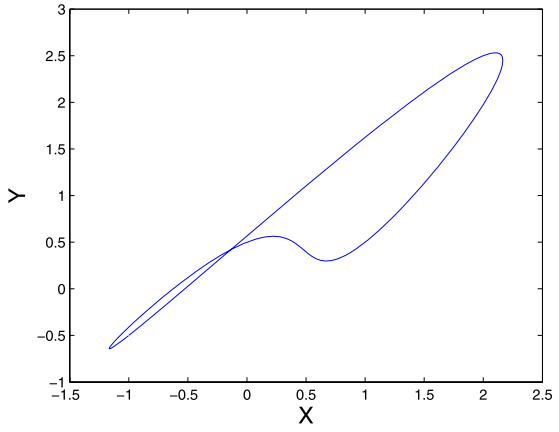

(b) Special affine transformation $\overline{\gamma}(t)$

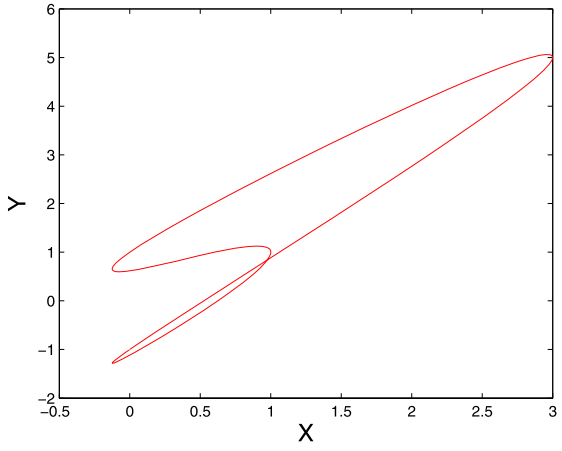

(c) Full affine transformation $\overline{\gamma_a(t)}$

Fig. 5 Dependence of invariants on re-parametrization: $\tau = \sqrt{t+1}$

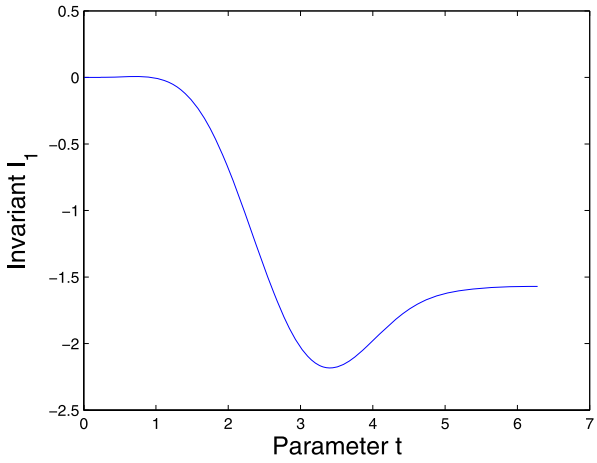

(a) Invariant I_1 for $\gamma(t)$ and $\overline{\gamma(t)}$

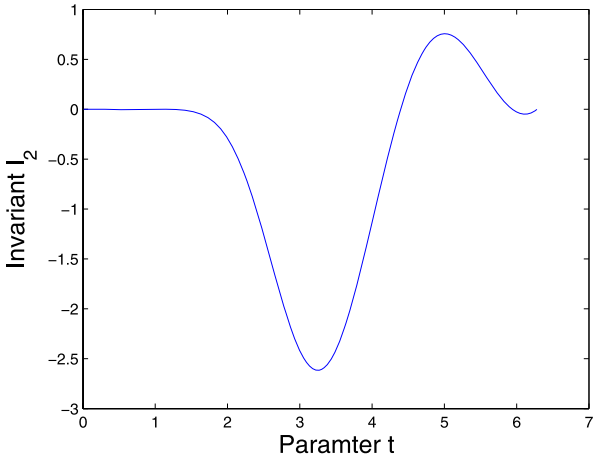

(b) Invariant I_2 for $\gamma(t)$ and $\overline{\gamma(t)}$

4.1 Global Integral Affine Signatures

A global integral signature of a curve is the variation of one independent integral invariant, evaluated on the curve, relative to another integral invariant. If a curve is mapped to another curve by a group transformation, their signatures coincide independently of the selected parametrization. The global signature, however, does depend on a choice of the initial point.

4.1.1 Global Affine Signature for Curves in $\mathbb{R}^2$

The special affine signature of a planar curve $\gamma(t)$ is constructed by, first, evaluating invariants I_1 and I_2 in (13) on this curve, and then plotting the parameterized curve $(I_1(t), I_2(t))$ in $\mathbb{R}^2$. For instance, the signature of the planar curve $\gamma(t)$ shown in Fig. 4a is a planar curve in Fig. 6. The signature of the curve $\overline{\gamma(t)}$ (Fig. 4b), which is related to $\gamma(t)$ by an affine

Fig. 5 (*Continued*)

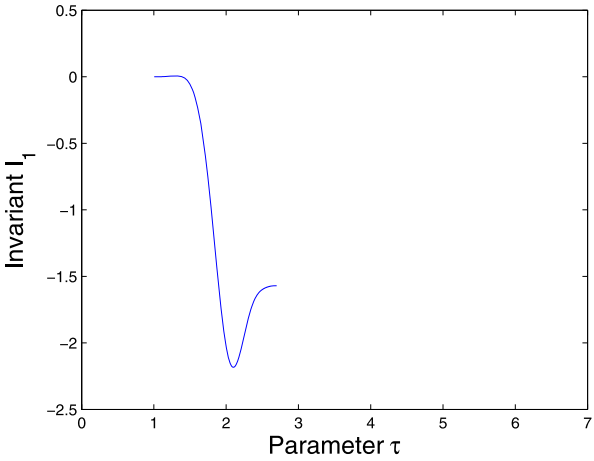

(c) Invariant I_1 for $\gamma(\tau)$ and $\overline{\gamma(\tau)}$

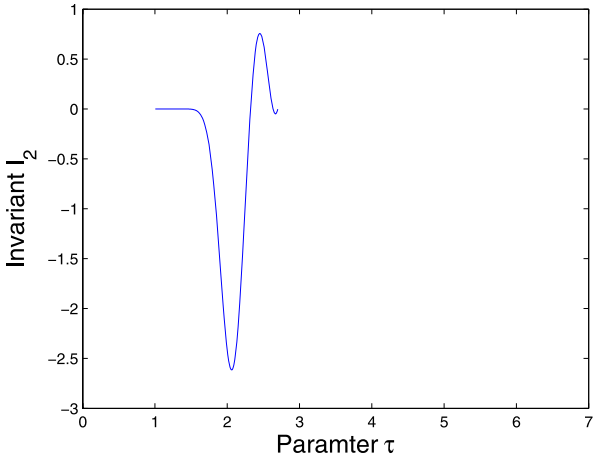

(d) Invariant I_2 for $\gamma(\tau)$ and $\overline{\gamma(\tau)}$

transformation, coincides with the signature of $\gamma(t)$. Moreover, it coincides with the signatures of reparametrized curves $\gamma(\tau)$ and $\overline{\gamma(\tau)}$.

Similarly, a full affine signature can be defined as a parameterized planar curve $(I_2^{\mathcal{A}}, I_3^{\mathcal{A}})$ defined by invariants in (15). Alternatively, we can use the two special affine invariants to cancel the effects of reflections and arbitrary scalings,

$$\tilde{I}_1(t) = \frac{|I_1(t)|}{\max_t |I_1|}, \qquad \tilde{I}_2(t) = \frac{|I_2|}{\max_t (I_1^2)}. \tag{23}$$

Both invariants are reduced relative to the range of $|I_1|$. The range of $\tilde{I}_1$ is from 0 to 1. It is not difficult to show that $\max_t |I_1| = 0$ on γ if and only if γ is a straight line. In this case $\tilde{I}_1(t)$ and $\tilde{I}_2(t)$ are undefined, but straight line regions can be easily detected by other means.

The full affine signature of a plane curve $\gamma(t)$ is obtained by, first, evaluating $\tilde{I}_1$ and $\tilde{I}_2$ on this curve and by then plotting the parameterized curve $(\tilde{I}_1(t), \tilde{I}_2(t))$ in $\mathbb{R}^2$. For example,

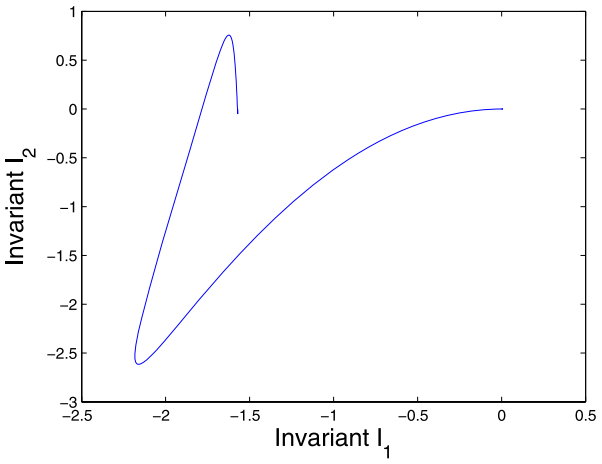

Fig. 6 Signatures for $\gamma(t)$, $\overline{\gamma(t)}$,$\gamma(\tau)$, and $\overline{\gamma(\tau)}$ coincide

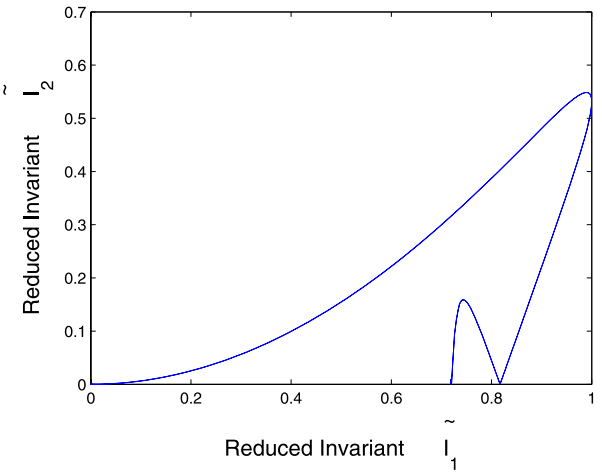

Fig. 7 Full affine signatures for curves $\overline{\gamma(t)}$ and $\overline{\gamma_a(t)}$ coincide

curves in Fig. 4a and c are related by a non-area-preserving affine transformation. Their full affine signatures coincide as shown on Fig. 7.

4.1.2 Global Affine Signatures for Curves in $\mathbb{R}^3$

To construct special affine signatures for spatial curve we use invariants J_1 and J_2 given by (21). Similarly to 2D case, the special affine signature of a spatial curve $\beta(t)$ is obtained by, first, evaluating J_1 and J_2 on this curve, and then plotting the parameterized curve $(J_1(t), J_2(t))$ in $\mathbb{R}^2$.

For example, the signature of a spatial curve $\beta(t) = (\sin t - 1/5\cos^2 t + 1/5, 1/2\sin t - \cos t + 1, \sin^2 t + \cos t - 1)$, shown in Fig. 8a, is the plane curve shown on Fig. 9. A curve $\overline{\beta(t)}$ is obtained from β by a special affine transformation

$$\begin{pmatrix} 0.3816 & 0.7631 & 1.1447 \\ 1.9079 & 1.5263 & 2.2894 \\ 2.6710 & 3.0526 & 3.4341 \end{pmatrix}.$$

Fig. 8 Spatial curve β and its transformations

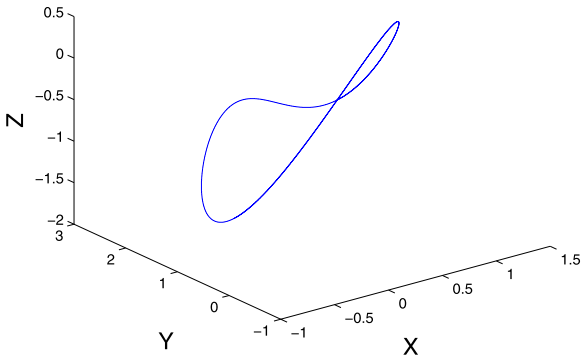

(a) Original curve $\beta(t)$

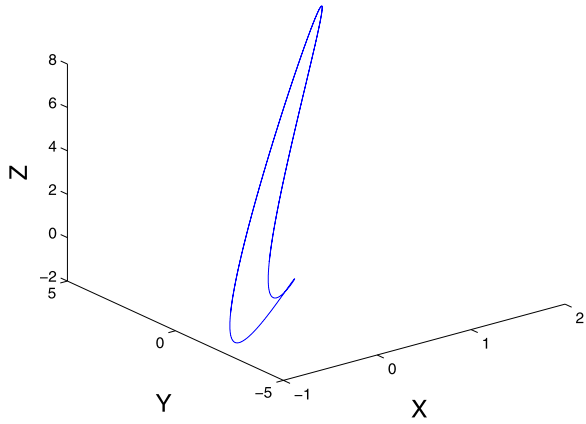

(b) Special affine transformation $\overline{\beta(t)}$

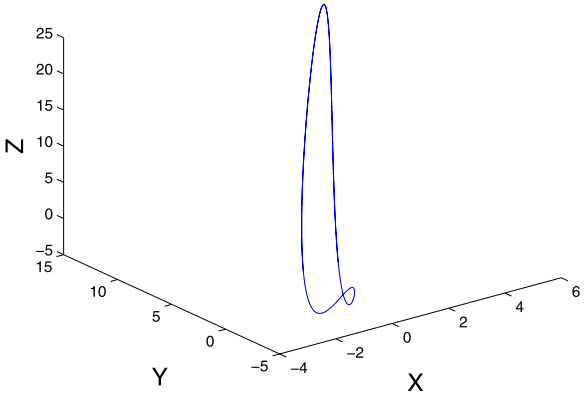

(c) Full affine transformation $\overline{\beta_a(t)}$

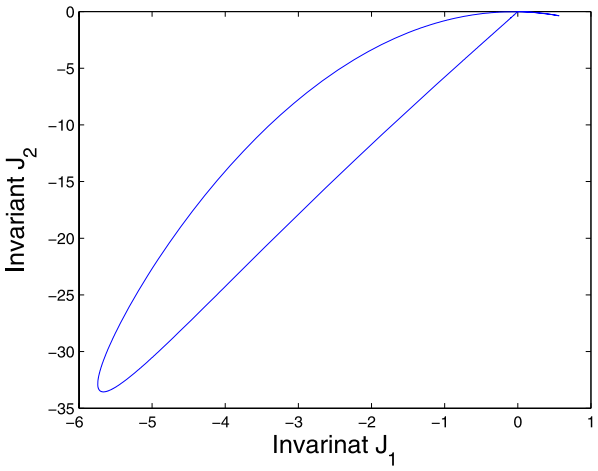

Fig. 9 Signatures for $\beta(t)$ and $\overline{\beta(t)}$ coincide

A curve $\overline{\beta_a(t)}$ is obtained from β by a full affine transformation

$$\begin{pmatrix} 1 & 2 & 3 \\ 4 & 5 & 6 \\ 9 & 8 & 7 \end{pmatrix}.$$

As Fig. 9 illustrates, the special affine signatures of $\beta(t)$ and $\overline{\beta(t)}$ coincide.

Similar to the 2D case, the full affine signature for curves in 3D is obtained by reducing special affine invariants J_1 and J_2 by the range of $|J_1|$

$$\tilde{J}_1(t) = \frac{|J_1(t)|}{\max_t |J_1|}, \qquad \tilde{J}_2(t) = \frac{J_2(t)}{\max_t (J_1^2)}. \tag{24}$$

The full affine signature of a spatial curve $\beta(t)$ is obtained by first evaluating $\tilde{J}_1$ and $\tilde{J}_2$ on this curve, and by then plotting the parameterized curve $(\tilde{J}_1(t), \tilde{J}_2(t))$ in $\mathbb{R}^2$. The full affine signatures of β, $\bar{\beta}$ and $\bar{\beta}_a$ coincide as shown in Fig. 10.

The advantage of global signatures is their independence of parametrization, whereas the result of evaluation of invariants J_1 and J_2 on a curve depends on the choice of parametrizations similarly to I_1 and I_2 in 2D case. The disadvantage of global signatures is in their dependence on the choice of the initial point of a curve. The local signature construction in the next section overcomes this dependence.

4.2 Local Integral Affine Signatures

The signatures defined in the previous section can not be used for classification unless the initial point of a curve is known. This becomes an obstacle for comparing closed curves or for matching partial contours. For illustration, let us choose two different initial points, a black circle or a red star, on the planar curve in Fig. 11. The resulting global affine signatures are different as illustrated in Figs. 12a and b. We overcome the dependence on the initial point by introducing local signatures. To proceed with the construction of the local signature, we replace the integration from the initial point with integration on local segments. To retain affine invariant properties of the signatures, we need to partition the curve in an invariant

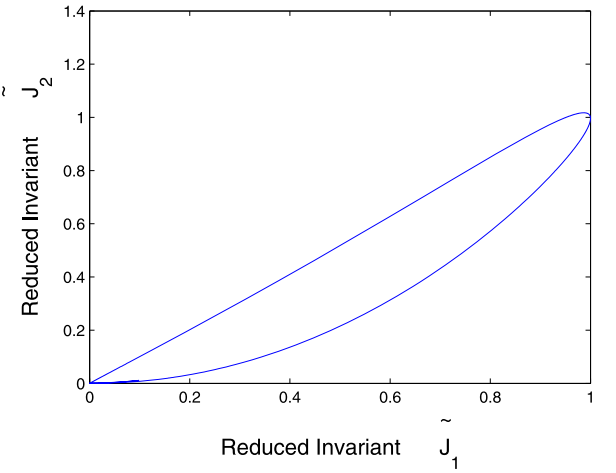

Fig. 10 Full affine signatures for $\beta(t)$, $\overline{\beta(t)}$, $\overline{\beta_a(t)}$

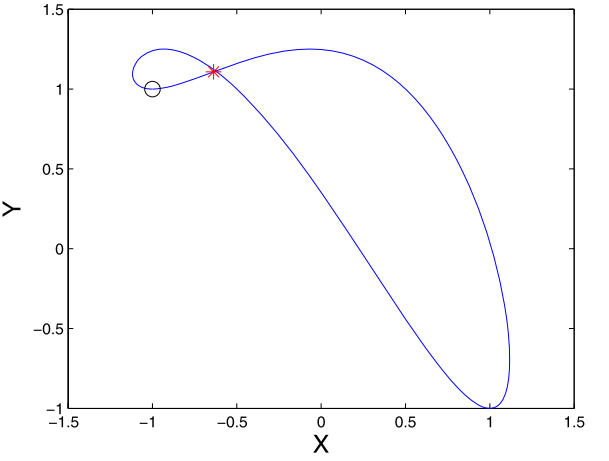

Fig. 11 A planar curve with two different choices of the initial points

manner. Such partition can be achieved using the notion of affine arc-length from classical differential geometry. Our goal, however, is to propose a derivative free method, and so we use the lowest order integral invariants, namely I_1 for plane curves and J_1 for spatial curve to obtain an equi-affine partition of a given curve. The details are described in the following subsections.

4.2.1 Local Affine Signatures for Curves in $\mathbb{R}^2$

We will use I_1 to partition a given curve into equi-affine sub-segments. Assume that γ is parametrized by $t \in [0, 1]$. Recall that the integration in the integral variables is performed from the initial point $\gamma(0)$ to a current point on the curve $\gamma(t)$. For instance, $I_1(t) = \int_0^t XdY - \frac{1}{2}XY$, where $X = x(t) - x(0)$ and $Y = y(t) - y(0)$. Thus $I_1(t)$ is a function from $[0, 1]$ to $\mathbb{R}$.

We define the evaluation of an invariant on a sub-segment of γ by treating the starting point of the sub-segment as the initial point, and computing the value of integral variables at

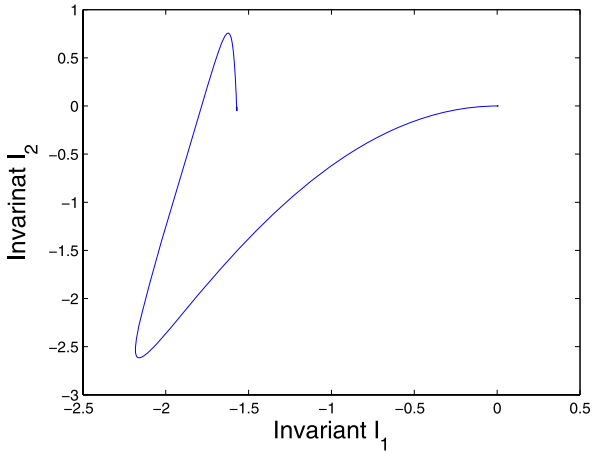

(a) Initial point is the black circle in Fig. 11

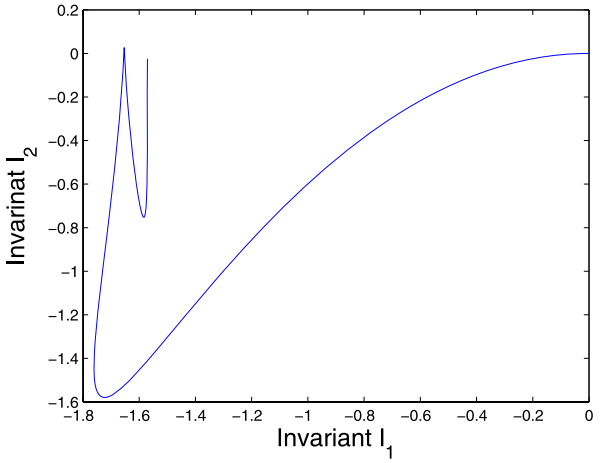

(b) Initial point is the red star in Fig. 11

Fig. 12 Global signatures for the same curve with two different choices of the initial point

its end point. In particular, for a sub-segment defined by the parameter range $[p, q] \subset [0, 1]$, we compute the evaluation $I_1^{[p,q]} = \int_p^q (x(t) - x(p))dy(t) - \frac{1}{2}(x(q) - x(p))(y(q) - y(p))$, and similarly for invariants I_2 and I_3 defined by (13). We note that the evaluation of an invariant on a segment is a real number.

We choose a sufficiently small $\Delta > 0$ and define an equi-affine partition $0 = t_0 < t_1 < \cdots < t_N = 1$ of the curve $\gamma(t), t \in [0, 1]$ into sub-segments by the condition

$$\left| I_1^{[t_{i-1},t_i]} \right| = \Delta. \tag{25}$$

In practice we choose Δ proportionally to the maximum of the absolute value of I_1, i.e., we choose an integer M and set $\Delta = \frac{\max_t |I_t|}{M}$. Note that the total number N of segments that we obtain using condition (25) differs from M in general. The *local discrete special*

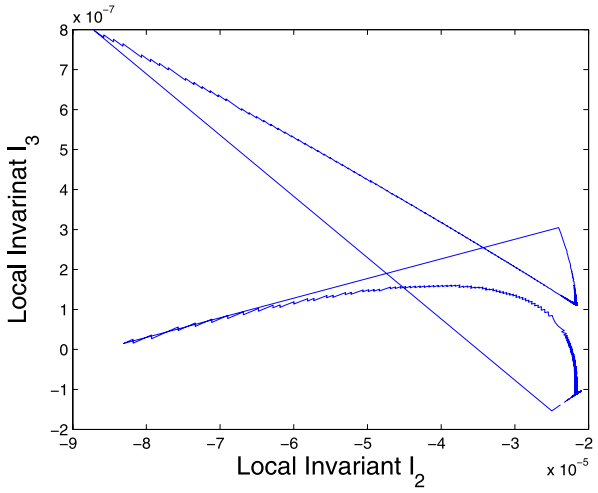

Fig. 13 Local special affine signature for the curve shown on Fig. 11

affine signature of γ is defined by the evaluation of I_2 and I_3 on the intervals $[t_{i-1}, t_i]$, $i = 1, \ldots, N$, that is a set of points with coordinates $(I_2^{[t_{i-1},t_i]}, I_3^{[t_{i-1},t_i]})$, $i = 1, \ldots, N$. Figure 13 shows the local discrete special affine signature for the curve shown in Fig. 11. The signature does not depend on a choice of the starting point. To obtain *local discrete affine signature* of γ, we use reduced invariants, that is we plot $(\frac{I_2^{[t_{i-1},t_i]}}{\max_t (I_1^2)}, \frac{I_3^{[t_{i-1},t_i]}}{\max_t |I_1^3|})$, $i = 1, \ldots, N$.

4.2.2 Local Affine Signatures for Curves in $\mathbb{R}^3$

For spatial curves we proceed in a similar manner as for planar curves. We use invariant J_1 to partition a curve $\gamma(t), t \in [0, 1]$ into N sub-intervals defined by $a = t_0 < t_1 < \cdots < t_N = b$ such that $J_1^{[t_{i-1},t_i]} = \Delta, i = 1, \ldots, N$, where $\Delta > 0$ is proportional to the maximum of the absolute value of J_1. We define a local special affine signature by evaluation of J_2 and J_3 on the intervals $[t_{i-1}, t_i], i = 1, \ldots, N$, that is by a set of points on the plane with coordinates $(J_2^{[t_{i-1},t_i]}, J_3^{[t_{i-1},t_i]})$, $i = 1, \ldots, N$.

Figure 14b shows the local special affine signature for a curve shown on Fig. 14a. The signature does not depend on our choice of initial point.

5 Application to 3D Object Classification

The features of many computer vision and pattern analysis problems are spatial curves. We can hence view the classification problem as that of assorting the similarity of curves in 3D, in particular, when subjected to affine transformations. In this section, we apply integral special affine invariants J_1 and J_2, the global special affine signature, and the local special affine signature to classify curves in 3D under special affine transformations. The performance of each of the proposed methods is evaluated. Applying these invariants to classification of 3D objects based on a set of characteristic spatial curves is in line of [2], and will be considered in subsequent publications.

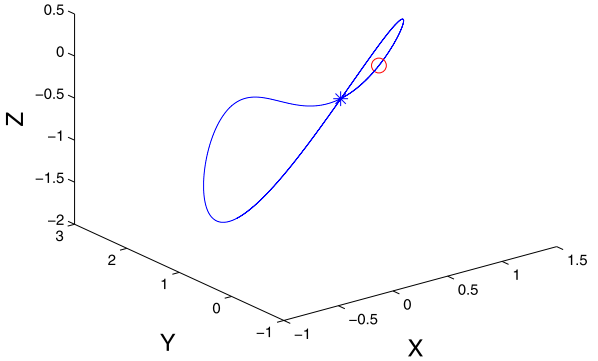

(a) A curve with two different choices of an initial point

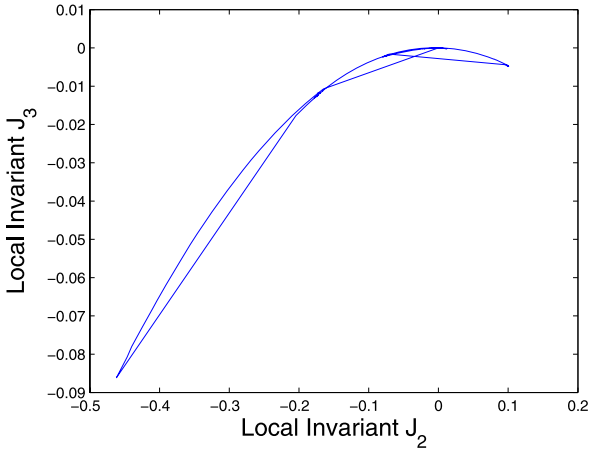

(b) Local special affine signature

Fig. 14 A spatial curve and its local special affine signature

5.1 Experimental Design

The Princeton Shape Benchmark [20] provides a repository of 3D models. A subset of three models are shown in Fig. 15. We extract a total of 100 characteristic curves, and each of them are re-sampled to 5000 points with the same arclength. We applied to each curve 9 randomly generated 3D special affine transformations as shown on (Fig. 16). To make this problem even more challenging and to illustrate the noise sensitivity of the proposed approach, Gaussian noise with distribution $N(0, \sigma^2)$ is added to each of the variations. We therefore obtain a classification set of 900 curves that has to be separated into 100 equivalent classes under affine transformations. The training set consists of 100 original curves without any noise and transformation. The discrimination power and sensitivity to noise are analyzed using the error rate of classification. We implemented a Nearest Neighbour (NN) classifier in a Euclidean space using Euclidean distance. In order to illustrate the advantages of the signature construction, we design two experiments. The first experiment uses a common parametrization for both the training and testing curves, while in the second experiment, we choose two different parametrizations (samplings) for the testing data.

Fig. 15 3D models from the Princeton shape benchmark

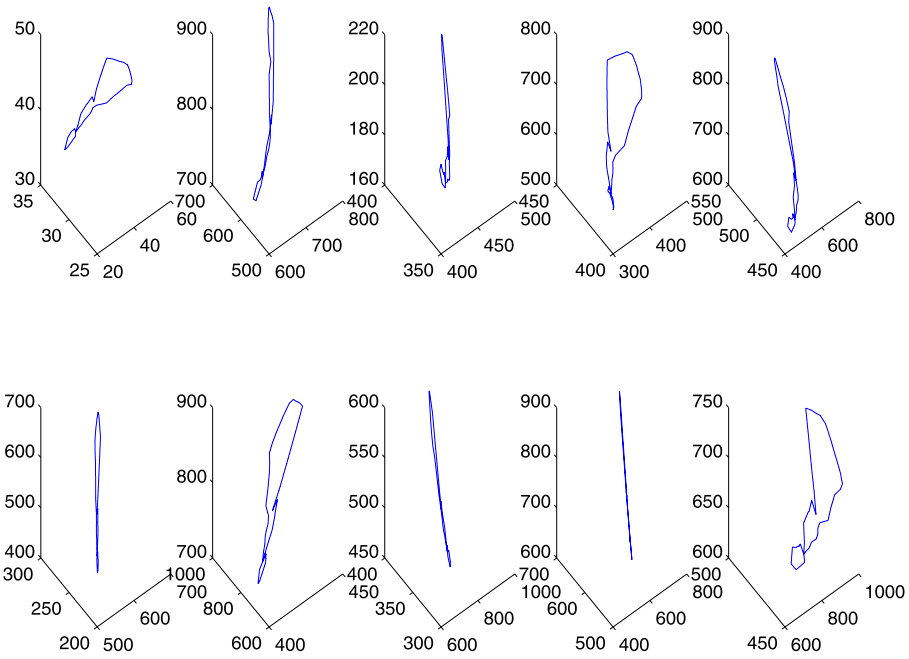

Fig. 16 A curve and 9 variations of it under affine transformation

5.2 Experimental Results

Three experiments are carried out with different noise variance, namely $\sigma = 2$ (Fig. 17), $\sigma = 1$, and $\sigma = 0.5$.

In the first experiment curves in testing and training sets had the same parameterization. The classification error rates for the three different values of sigma are shown in Table 1. Both the integral invariants and the signatures perform well as indicated by the error rates. For comparison, the classical differential invariants have a classification error rate more then 80%, which makes the differential invariants practically useless. Since the order of integral variables involved in J_2 is higher than J_1, as well as the explicit form of J_2 is more complicated than J_1, the performance of J_2 is not as good as that of J_1. The global signature is constructed with both J_1 and J_2, and the local signature is based on J_2 and J_3. The performance of these signatures is therefore slightly worse than J_2.

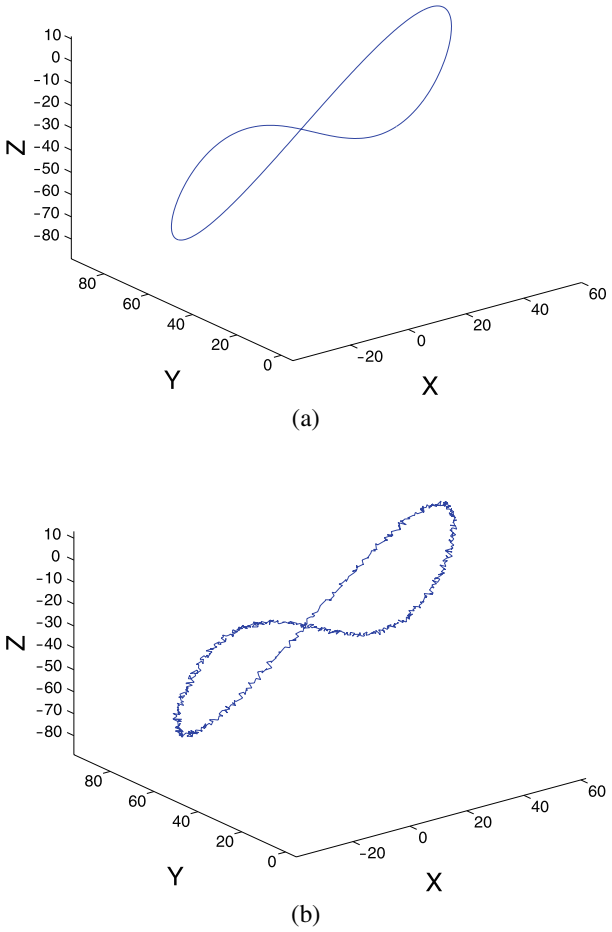

Fig. 17 (**a**) A spatial curve without noise (**b**) with Gaussian noise $N(0, 4)$

Table 1 Classification error rate with same parametrization, same initial points

Noise variance	J_1	J_2	Global signature	Local signature
$\sigma = 0.5$	**0.0022**	0.0472	0.06	0.07
$\sigma = 1$	**0.04**	0.12	0.15	0.17
$\sigma = 2$	**0.0789**	0.2233	0.28	0.32

If the parameterizations are not the same, the plots of invariants J_1 and J_2 with respect to a parameter can not be used for a classification purpose as illustrated in Table 2. Even with the lowest noise variance, the error rates are more than 0.4 for J_1 and 0.6 for J_2. However, neither the global signature nor local signature are affected.

Table 2 Classification error rate with different parametrization, same initial points

Noise variance	J_1	J_2	Global signature	Local signature
$\sigma = 0.5$	*0.42*	*0.61*	**0.06**	**0.07**
$\sigma = 1$	*0.48*	*0.70*	**0.15**	**0.17**
$\sigma = 2$	*0.56*	*0.83*	**0.28**	**0.32**

Table 3 Classification error rate with different parametrization, different initial points

Noise variance	J_1	J_2	Global signature	Local signature
$\sigma = 0.5$	*0.87*	*0.95*	*0.95*	**0.07**
$\sigma = 1$	*0.91*	*0.97*	*0.97*	**0.17**
$\sigma = 2$	*0.94*	*0.98*	*0.98*	**0.32**

If we make an arbitrary selection of the initial points, both individual invariants (J_1 and J_2) and global signature have poor performance as shown in Table 3. Only local signature may be used to characterize a curve.

In summary, if the training data and testing data have similar parameterization and same initial point, either invariants or signatures may be used. Under different parametrization, the global signature is the best choice. In the case when the starting point is undefined one needs to use local signature.

6 Conclusion

In this paper we presented explicit formulae for affine integral invariants for planar and spatial curves in terms of Euclidean invariants, and introduced signatures based on these invariants. Two curves that are equivalent with respect to affine group of transformation have the same signature. Although we have focused here on a larger group of the affine transformations, the integral Euclidean invariants, presented here, can be used to classify curves under Euclidean transformations with the analogous signature constructions.

Integral invariants are functions of a parameter and hence depend on the parameterization (curve sampling). The signatures, based on these invariants, are independent of parameterization. Global integral signatures depend on a choice of the initial point. Local integral signatures provide a classification method independent of the choice of the initial point, and so they can hence be used on images with occlusions and for comparing fragments of contours. They are slightly more sensitive to noise than global signatures.

Our interest in noise tolerant integral invariants for spatial curves is motivated by an increasing availability of 3D data acquisition systems and subsequent emerging interest in 3D image analysis. As an experiment, a classification of characteristic curves of 3D objects, subjected to random affine transformations and noise, was conducted by using individual invariants, and global and local signatures. Integral invariants allow us to perform noise tolerant classification of curves with respect to affine transformations (for comparison: differential invariants give 80% error rate).

Substantial further experiments in this direction and comparison of the proposed method with numerous other approaches is the subject of our current and future work. In particular, we would like to compare the performance of our methods with methods based on

the following approaches. Arbter et al. [3] applied affine-invariant Fourier descriptors to the problem of 3D object recognition. More specifically, affine-invariant Fourier descriptors were applied to planar feature-curves extracted from a 3D object. Tieng and Boles [35] introduced a wavelet based affine-invariant representation for planar objects. Sener and Unel [32] used principal component analysis (PCA) and independent component analysis (ICA). Wang and Teoh [39] developed an affine invariant approach to model planar curves in B-spline model and to match curves in curvature scale space. Note, however, that in all these cases, the affine classification methods were limited to *planar* curves. Our literature-search indicated that the present paper is the first to introduce a noise tolerant method for the affine curve-matching in 3D.

Understanding theoretical properties of integral invariants introduced in this paper, in particular, establishing the structure of the entire set of these invariants, as well as extensions to higher dimensions and other groups are of interest.

Appendix: Derivation of Invariants

7.1 Cross-section and Moving Frame Map

Building on the works [15, 16, 21], Fels and Olver [11] generalized Cartan's normalization procedure [7], and proposed a general algorithm for computing invariants. The Fels-Olver algorithm relies on a map $\rho\colon S \to G$ with an *equivariant* property:

$$\rho(g \cdot s) = \rho(s) \cdot g^{-1}, \quad \forall g \in G,\ \forall s \in S. \tag{26}$$

From Theorem 4.4 in [11], it follows that such map exists if and only if the action of G is free and, in addition, there exists a global *cross-section*, i.e. a subset $\mathcal{K} \subset S$ that intersects each orbit O_s at a unique point. Indeed, under the above assumption the map ρ may be defined by the condition $\rho(s) \cdot s \in \mathcal{K}$. Then $\rho(s) \cdot s = \rho(g \cdot s) \cdot (g \cdot s)$ is the unique point of the intersection of O_s and $\mathcal{K}$. Since the action assumed to be free it follows that s may be "cancelled" and hence the condition (26) is satisfied.

If G is a Lie group acting smoothly on $\mathbb{R}^n$ and both $S \subset \mathbb{R}^n$ and $\mathcal{K} \subset S$ are smooth submanifolds, then $\mathbb{R}^n$-coordinate components of the projection $\iota(s) = \rho(s) \cdot s\colon S \to \mathcal{K}$ are smooth invariant functions, called normalized invariants. Normalized invariants contain a maximal set of functionally independent invariants, and have a *replacement property*, which allows us to rewrite any invariant in terms of them by simple substitution [11, 18, 19].

Although, a global smooth cross-section does not always exist, a local smooth cross-section[4] passing through every point of S can be found for every semi-regular action.[5] The freeness assumption can be also relaxed to a semi-regularity assumption. With these weaker assumptions the above method can be used to construct local invariants [11, 19].[6]

For algebraic groups acting on algebraic varieties, a purely algebraic counterpart of the Fels-Olver construction was obtained in [18, 19]. The algebraic method can be combined with the inductive approach described below. In some particular examples, including the 3D

[4] A local cross-section is defined on an open subset of $U \subset S$ and $\forall s \in U$ intersects each connected component of $O_s \cap U$ at a unique point.

[5] An action of G is called *semi-regular* if all orbits have the same dimension.

[6] A function f, defined on an open subset U of S, is a *local invariant* if $\forall s \in U$ there exists an open neighborhood G_s of $e \in G$ s.t. condition (1) is satisfied for all $g \in G_s$.

example presented here, the computation based on the moving frame map ρ turns out to be more practical.

When the group G is of a relatively large dimension, computation of invariants by either a geometric or algebraic approach becomes challenging. In [22] two modifications of the moving frame method were proposed to simplify the computation by splitting it into two steps: invariants of a subgroup $A \subset G$ are first computed, and then invariants of the entire group are constructed in terms of those. For the problem at hand, we use one of these modifications, called the inductive approach, which is applicable when a group factors into a product of two subgroups.

7.2 Inductive Approach

Definition 7.1 A group G *factors as a product* of its subgroups A and B if for any $g \in G$ there are $a \in A$ and $b \in B$ such that $g = ab$.

We write $G = A \cdot B$. If in addition $A \cap B = e$, then for each $g \in G$ there are *unique* elements $a \in A$ and $b \in B$ such that $g = ab$.

From Theorem 4.4 in [22] it follows that if $G = B \cdot A$, such that $A \cap B$ is discrete, and G acts freely on a manifold S then $\forall s \in S$ there exists a local cross-section $\mathcal{K}_A$, containing s, invariant under the action of the subgroup B. From Lemma 4.7 in [22] it follows that invariants of G can be constructed from the invariants of A using the following method.

Inductive method

1. Restrict the G-action to A. Find a local cross-section $\mathcal{K}_A \subset S$ for the action of A which is invariant under the action of B.
2. Construct a moving frame map $\rho_A \colon S \to A$ defined by the condition $\rho_A(s) \cdot s \in \mathcal{K}_A$, $\forall s \in S$, by solving the corresponding equations. Composition of coordinate functions with the projection $\iota(s) = \rho_A(s) \cdot s \colon S \to \mathcal{K}_A$ are invariant with respect to the action of A.
3. Restrict the action of G to the action of its subgroup B on the invariant subset $\mathcal{K}_A$ and choose a local cross-section $\mathcal{K}_B \subset \mathcal{K}_A$.
4. Construct a moving frame map $\rho_B \colon \mathcal{K}_A \to B$ defined by the condition $\rho_B(s) \cdot z \in \mathcal{K}_B, \forall z \in \mathcal{K}_A$, by solving the corresponding equations.
5. The G-moving frame map $\rho \colon S \to G$ is defined by $\rho(s) = \rho_B(\rho_A(s) \cdot s)\rho_A(s)$, and G-invariants are the coordinate components of $\rho(s) \cdot s = \rho_B(\rho_A(s) \cdot s) \cdot (\rho_A(s) \cdot s) = \rho_B(\iota_A(s)) \cdot \iota_A(s)$.

7.3 Affine Integral Invariants for Curves in $\mathbb{R}^2$

We have a product decomposition $SL(2) = B \cdot A$, where $B = \{\left(\begin{smallmatrix} b_{11} & b_{12} \\ 0 & \frac{1}{b_{11}} \end{smallmatrix}\right) | b_{11} > 0\}$ and $A = SO(2)$ is a group of rotations. The intersection $B \cap A = \{e\}$, and therefore we can apply the inductive method as follows.

1. We restrict the $SL(2)$-action (11) to the subgroup $\mathcal{S}O(2)$ of the rotation matrices by setting $a_{11} = \cos\phi, a_{12} = -\sin\phi, a_{21} = \sin\phi, a_{22} = \cos\phi$. A subset $\mathcal{K}_A$ defined by conditions $Y = 0, X > 0$ serves as a cross-section on an open subset of the integral jet bundle. Moreover $\mathcal{K}_A$ is invariant under the restriction of (11) to subgroup B.

2. The corresponding moving frame map

$$\rho_A(s) = \begin{pmatrix} \frac{X}{\sqrt{X^2+Y^2}} & \frac{Y}{\sqrt{X^2+Y^2}} \\ -\frac{Y}{\sqrt{X^2+Y^2}} & \frac{X}{\sqrt{X^2+Y^2}} \end{pmatrix}$$

is obtained by solving the equation $\overline{Y} = 0$ with the condition $\overline{X} > 0$ (see the first line of (11)). The projection $\iota_A \colon \mathbb{R}^5 \to \mathcal{K}_A$, obtained by substitution ρ_A into (11), produces a point whose coordinates are invariant under the action of $\mathcal{SO}(2)$. Non-constant normalized invariants are given by (12) and $Y_{SE} = 0$ is the remaining constant invariant.

3. We now restrict the action (11) to the action of a subgroup B on an invariant subset $\mathcal{K}_A$. We obtain the following transformations.

$$\begin{aligned} \overline{X_A} &= b_{11} X_A, & \overline{Y_A^{[1,0]}} &= Y_A^{[1,0]}, \\ \overline{Y_A^{[1,1]}} &= \frac{1}{b_{11}} Y_A^{[1,1]}, & \overline{Y_A^{[2,0]}} &= b_{11} Y_A^{[2,0]} + 2 b_{12} Y_A^{[1,1]}, \\ \overline{Y_A^{[1,2]}} &= \frac{1}{b_{11}^2} Y_A^{[1,2]}, & \overline{Y_A^{[2,1]}} &= Y_A^{[2,1]} + 2 \frac{b_{12}}{b_{11}} Y_A^{[1,2]}, \\ \overline{Y_A^{[3,0]}} &= b_{11}^2 Y_A^{[3,0]} + 3 b_{12}^2 Y_A^{[1,2]} + 3 b_{11} b_{12} Y_A^{[2,1]}. \end{aligned} \tag{27}$$

A subset $\mathcal{K}_B \subset \mathcal{K}_A$ defined by the equations $X_A = 1$, $Y_A^{[2,0]} = 0$ serves as a cross-section on the subset of $\mathcal{K}_A$, where $Y_A^{[1,1]} \neq 0$.

4. This leads to the moving frame map

$$\rho_B(s) = \begin{pmatrix} \frac{1}{X_A} & -\frac{Y_A^{[2,0]}}{2 Y_A^{[1,1]} X_A} \\ 0 & X_A \end{pmatrix}.$$

The projection $\iota_B \colon \mathcal{K}_A \to \mathcal{K}_B$, defined by $\iota_B(s) = \rho_B(s) \cdot s$, produces a point with coordinates

$$\begin{aligned} X_B &= 1, & Y_B^{[1,0]} &= Y_A^{[1,0]}, \\ Y_B^{[1,1]} &= X_A Y_A^{[1,1]}, & Y_B^{[2,0]} &= 0, \\ Y_B^{[1,2]} &= X_A^2 Y_A^{[1,2]}, & Y_B^{[2,1]} &= Y_A^{[2,1]} - \frac{Y_A^{[2,0]}}{Y_A^{[1,1]}} Y_A^{[1,2]}, \\ Y_B^{[3,1]} &= \frac{1}{X_A^2} \left(Y_A^{[3,0]} + \frac{3}{2} \frac{Y_A^{[2,0]}}{Y_A^{[1,1]}} Y_A^{[2,1]} + \frac{3}{4} \left(\frac{Y_A^{[2,0]}}{Y_A^{[1,1]}} \right)^2 Y_A^{[1,2]} \right), \end{aligned} \tag{28}$$

invariant under the B-action (27) on $\mathcal{K}_A$.

5. Replacing coordinates $Y_A^{[i,j]}$ with the corresponding $Y_{SE}^{[i,j]}$ given by (12) produces independent invariants (13).

7.4 Affine Integral Invariants for Curves in $\mathbb{R}^3$

We have a product decomposition $SL(3) = B \cdot A$, where

$$B = \left\{ \begin{pmatrix} b_{11} & b_{12} & b_{13} \\ 0 & b_{22} & b_{23} \\ 0 & 0 & \frac{1}{b_{11}b_{22}} \end{pmatrix} \Big| b_{11} > 0, b_{22} \neq 0 \right\}$$

and $A = SO(3)$ is a group of rotations. The intersection $B \cap A = \{e\}$ is trivial. We again follow the steps of the inductive method.

1. We restrict the $\mathcal{S}L(3)$-action (8) to the action of $\mathcal{S}O(3)$ whose elements can be represented as the product of three rotations:

$$\begin{pmatrix} 1 & 0 & 0 \\ 0 & \cos\psi & -\sin\psi \\ 0 & \sin\psi & \cos\psi \end{pmatrix} \begin{pmatrix} \cos\phi & 0 & \sin\phi \\ 0 & 1 & 0 \\ -\sin\phi & 0 & \cos\phi \end{pmatrix} \begin{pmatrix} \cos\theta & -\sin\theta & 0 \\ \sin\theta & \cos\theta & 0 \\ 0 & 0 & 1 \end{pmatrix}.$$

   A subset $\mathcal{K}_A$ defined by conditions $Y = 0$, $Z = 0$, $Z^{[0,1,1]} = 0$, $X > 0$ serves as a cross-section on an open subset of the integral jet bundle where $X^2 + Y^2 + Z^2 > 0$. The cross-section $\mathcal{K}_A$ is invariant under the action of B.
2. The corresponding moving frame map ρ_A is obtained by solving the equation $\overline{Y} = 0$, $\overline{Z} = 0$, $\overline{Z^{[0,1,1]}} = 0$ with the condition $\overline{X} > 0$. Explicitly, let $r = \sqrt{X^2 + Y^2}$, $R = \sqrt{X^2 + Y^2 + Z^2}$ and $\Upsilon = \sqrt{(Z_R^{[0,2,0]})^2 + 4(Z_R^{[0,1,1]})^2}$, where $Z_R^{[0,1,1]}$ and $Z_R^{[0,2,0]}$ are given on the last page of the Appendix, then

$$\begin{aligned} &\cos\theta = \frac{X}{r}, \qquad \cos\phi = \frac{r}{R}, \qquad \cos\psi = \frac{Z_R^{[0,2,0]}}{\Upsilon}, \\ &\sin\theta = -\frac{Y}{r}, \qquad \sin\phi = \frac{Z}{R}, \qquad \sin\psi = -2\frac{Z_R^{[0,1,1]}}{\Upsilon}. \end{aligned} \tag{29}$$

   The corresponding set of $\mathcal{S}O(3)$ invariants is given by (19).
3. We now restrict the $\mathcal{S}L(3)$-action to the action of a subgroup B on an invariant subset of $\mathcal{K}_A$. We obtain the following transformations:

$$\begin{aligned} \overline{X_A} &= b_{11} X_A, \\ \overline{Z_A^{[0,1,0]}} &= \frac{1}{b_{11}} Z_A^{[0,1,0]}, \\ \overline{Z_A^{[1,0,0]}} &= \frac{1}{b_{22}} Z_A^{[1,0,0]} + \frac{b_{12}}{b_{11}b_{22}} Z_A^{[0,1,0]}, \\ \overline{Y_A^{[1,0,0]}} &= b_{11}b_{22} Y^{[1,0,0]} - b_{13}b_{22} Z_A^{[0,1,0]} + b_{11}b_{23} Z_A^{[1,0,0]} + b_{12}b_{23} Z_A^{[0,1,0]}, \\ \overline{Z_A^{[0,2,0]}} &= \frac{b_{22}}{b_{11}} Z_A^{[0,2,0]}, \\ \overline{Z_A^{[1,0,1]}} &= \frac{1}{b_{11}b_{22}^2} Z_A^{[1,0,1]}, \end{aligned}$$

$$\overline{Z_A^{[1,1,0]}} = Z_A^{[1,1,0]} + \frac{b_{23}}{b_{22}} Z_A^{[1,0,1]} + \frac{b_{12}}{b_{11}} Z_A^{[0,2,0]},$$

$$\overline{Y_A^{[1,0,1]}} = Y_A^{[1,0,1]} + \frac{b_{23}}{b_{22}} Z_A^{[1,0,1]} - \frac{b_{12}}{2b_{11}} Z_A^{[0,2,0]}.$$

A subset $\mathcal{K}_B \subset \mathcal{K}_A$ defined by equations

$$Z_A^{[0,1,0]} = 1, \qquad Z_A^{[1,0,0]} = 1, \qquad Y_A^{[1,0,0]} = 1, \qquad Z_A^{[0,2,0]} = 1, \qquad Z_A^{[1,1,0]} = 1$$

is a cross-section on an open subset of $\mathcal{K}_A$.

4. The corresponding moving frame map ρ_B is

$$b_{11} = Z_A^{[0,1,0]}, \qquad b_{12} = -\frac{Z_A^{[0,2,0]} Z_A^{[1,0,0]} - Z_A^{[0,1,0]}}{Z_A^{[0,2,0]}},$$

$$b_{22} = \frac{Z_A^{[0,1,0]}}{Z_A^{[0,2,0]}}, \qquad b_{23} = \frac{-Z_A^{[0,1,0]} Z_A^{[1,1,0]} + Z_A^{[0,2,0]} Z_A^{[1,0,0]}}{Z_A^{[0,2,0]} Z_A^{[1,0,1]}},$$

$$b_{13} = \frac{1}{Z_A^{[0,2,0]} Z_A^{[1,0,1]} Z_A^{[0,1,0]^2}} (Z_A^{[0,1,0]^2} Z_A^{[0,2,0]} Z_A^{[1,0,0]} - Z_A^{[0,1,0]^3} Z_A^{[1,1,0]}$$
$$+ Z_A^{[0,2,0]} Z_A^{[1,0,1]} Z_A^{[0,1,0]^2} Y_A^{[1,0,0]} - Z_A^{[1,0,1]} Z_A^{[0,2,0]^2}).$$

The coordinate components of the projection $\rho_B(s) \cdot s \colon \mathcal{K}_A \to \mathcal{K}_B$

$$X_B = Z_A^{[0,1,0]} X_A,$$

$$Z_B^{[1,0,1]} = \frac{Z_A^{[1,0,1]} Z_A^{[0,2,0]^2}}{Z_A^{[0,1,0]^3}},$$

$$Y_B^{[1,0,1]} = \frac{2Y_A^{[1,0,1]} Z_A^{[0,1,0]} - 2Z_A^{[0,1,0]} Z_A^{[1,1,0]} + 3Z_A^{[0,2,0]} Z_A^{[1,0,0]}}{2Z_A^{[0,1,0]}} - \frac{1}{2}$$

are invariant under the action of B on $\mathcal{K}_A$.

5. Replacing $X_A, Y_A^{[i,j,k]}, Z_A^{[i,j,k]}$ with $X_{SE}, Y_{SE}^{[i,j,k]}, Z_{SE}^{[i,j,k]}$ given by (19) produces independent invariants (20).

The following auxiliary expressions were used in the paper where $r = \sqrt{X^2 + Y^2}$, $R = \sqrt{X^2 + Y^2 + Z^2}$:

$$Z_R^{[0,1,0]} = -\frac{1}{2R}\left(XYZ - 2XZ^{[0,1,0]} + 2YZ^{[1,0,0]} - 2ZY^{[1,0,0]}\right),$$

$$Z_R^{[1,0,0]} = -\frac{1}{2r}\left(X^2 Z - 2XZ^{[1,0,0]} + Y^2 Z - 2YZ^{[0,1,0]}\right),$$

$$Y_R^{[1,0,0]} = -\frac{1}{2rR}\left(YX^3 + XY^3 - 2Y^2 Y^{[1,0,0]} - 2ZYZ^{[1,0,0]} - 2X^2 Y^{[1,0,0]} + 2ZXZ^{[0,1,0]}\right),$$

$$Z_R^{[0,1,1]} = -\frac{1}{6rR}\left(2YX^3 Z^2 - 6X^3 Z^{[0,1,1]} + 6X^2 YZ^{[1,0,1]} - 6X^2 ZY^{[1,0,1]}\right.$$

$$
\begin{aligned}
&- 6XZ^{[0,1,1]}Y^2 + 3XYZZ^{[0,2,0]} + 4Z^2Y^3X + 6XYZX^{[1,0,1]} \\
&- 6XZ^2X^{[1,1,0]} - 6Y^2ZZ^{[1,1,0]} - 6Y^2ZY^{[1,0,1]} + 6Y^3Z^{[1,0,1]} - 3Z^2YX^{[0,2,0]}\big),
\end{aligned}
$$

$$
\begin{aligned}
Z_R^{[0,2,0]} = &-\frac{1}{3rR}\big(-3X^2Z^{[0,2,0]} - 2Y^2X^2Z + 6XYZ^{[1,1,0]} + 3XZX^{[0,2,0]} \\
&+ 6Y^2X^{[1,0,1]} - 6ZYX^{[1,1,0]}\big),
\end{aligned}
$$

$$
\begin{aligned}
Z_R^{[1,0,1]} = &\frac{1}{6r^2R}\big(-4Z^2X^4 + 6Z^{[1,0,1]}X^3 + 6X^2YZ^{[0,1,1]} - 2X^2Z^2Y^2 + 6ZX^2X^{[1,0,1]} \\
&- 6XYZZ^{[1,1,0]} + 6XZ^{[1,0,1]}Y^2 - 3Y^2ZZ^{[0,2,0]} + 6Y^3Z^{[0,1,1]} - Z^2Y^4\big),
\end{aligned}
$$

$$
\begin{aligned}
Z_R^{[1,1,0]} = &\frac{1}{6r^2R^2}\big(6Z^2XYX^{[1,0,1]} - 6ZXY^2X^{[1,1,0]} - 3ZX^2YX^{[0,2,0]} + 6Z^2Y^2Y^{[1,0,1]} \\
&- 4ZX^5Y + ZY^5X + 6X^4Z^{[1,1,0]} - 6Y^4Z^{[1,1,0]} \\
&- 6ZYZ^{[1,0,1]}X^2 + 6ZXZ^{[0,1,1]}Y^2 + 3Z^2XYZ^{[0,2,0]} - 6ZX^3X^{[1,1,0]} \\
&- 3X^3Y^3Z + 12X^3YX^{[1,0,1]} + 12XY^3X^{[1,0,1]} \\
&- 6ZY^3Z^{[1,0,1]} + 6X^3YZ^{[0,2,0]} + 6XY^3Z^{[0,2,0]} + 6ZX^3Z^{[0,1,1]} \\
&- 6X^3Z^3Y + 6X^2Z^2Z^{[1,1,0]} + 6X^2Z^2Y^{[1,0,1]} - 3ZY^3X^{[0,2,0]} - 3Z^3Y^3X\big),
\end{aligned}
$$

$$
\begin{aligned}
Y_R^{[1,0,1]} = &-\frac{1}{6r^2R^2}\big(-6X^4Y^{[1,0,1]} - 12ZXY^2X^{[1,1,0]} + 6Z^2Y^2Y^{[1,0,1]} - 6Y^4Z^{[1,1,0]} \\
&- 6ZX^2YX^{[0,2,0]} - 6Y^2Z^{[1,1,0]}X^2 - 12ZYZ^{[1,0,1]}X^2 + 6Y^2Z^2Z^{[1,1,0]} \\
&- 12Y^2X^2Y^{[1,0,1]} - 6Y^4Y^{[1,0,1]} - 6ZY^3X^{[0,2,0]} - 12ZX^3X^{[1,1,0]} - 3Z^3Y^3X \\
&+ 9X^3Y^3Z + 4ZX^5Y - 12ZY^3Z^{[1,0,1]} + 12ZX^3Z^{[0,1,1]} + 3XY^3Z^{[0,2,0]} \\
&+ 5ZY^5X - 3Z^2XYZ^{[0,2,0]} + 12ZXZ^{[0,1,1]}Y^2 - 6Z^2XYX^{[1,0,1]} \\
&+ 6XY^3X^{[1,0,1]} + 6X^3YX^{[1,0,1]} + 6X^2Z^2Y^{[1,0,1]} + 3X^3YZ^{[0,2,0]}\big),
\end{aligned}
$$

$$
\begin{aligned}
X_R^{[1,1,0]} = &\frac{1}{6rR^2}\big(-Y^5X + 3Z^2Y^3X - 6ZY^2Y^{[1,0,1]} - 6ZX^2Y^{[1,0,1]} - 6ZY^2Z^{[1,1,0]} - 2X^5Y \\
&+ 6X^3X^{[1,1,0]} + 3XYZZ^{[0,2,0]} + 3X^2YX^{[0,2,0]} + 6XYZX^{[1,0,1]} + 6XY^2X^{[1,1,0]} \\
&+ 3Y^3X^{[0,2,0]} - 3X^3Y^3 - 6Z^2YZ^{[1,0,1]} + 6Z^2XZ^{[0,1,1]}\big),
\end{aligned}
$$

$$
\begin{aligned}
X_R^{[1,0,1]} = &\frac{1}{6rR}\big(-2ZX^4 + 6X^2X^{[1,0,1]} + 2Y^2X^2Z + 2X^2Z^3 - 6XYZ^{[1,1,0]} - 6ZXZ^{[1,0,1]} \\
&- 6ZYZ^{[0,1,1]} + 2Y^2Z^3 + Y^4Z - 3Z^{[0,2,0]}Y^2\big),
\end{aligned}
$$

$$
\begin{aligned}
X_R^{[0,2,0]} = &-\frac{1}{3r^2R}\big(-X^4Y^2 - Y^4X^2 - 3XY^2X^{[0,2,0]} - 3X^2Z^2Y^2 + 6Y^2ZX^{[1,0,1]} \\
&+ 6XYZZ^{[1,1,0]} - 3ZX^2Z^{[0,2,0]} + 6X^2YX^{[1,1,0]} - 3X^3X^{[0,2,0]} + 6Y^3X^{[1,1,0]}\big).
\end{aligned}
$$

References

1. Ames, A.D., Jalkio, J.A., Shakiban, C.: Three-dimensional object recognition using invariant Euclidean signature curves. In: Analysis, Combinatorics and Computing, pp. 13–23. Nova Sci. Publ., Hauppauge (2002)
2. Aouada, D., Feng, S., Krim, H.: Statistical analysis of the global geodesic function for 3D object classification. In: Proceedings of ICASSP, p. 11p, Honolulu, HI (2007)
3. Arbter, K., Snyder, W.E., Burkhardt, H., Hirzinger, G.: Application of affine-invariant Fourier descriptors to recognition of 3-D objects. IEEE Trans. Pattern Anal. Mach. Intell. **12**(7), 640–647 (1990)
4. Boutin, M.: Numerically invariant signature curves. Int. J. Comput. Vis. **40**, 235–248 (2000)
5. Bruckstein, A.M., Shaked, D.: Skew-symmetry detection via invariant signatures. Pattern Recogn. **31**, 181–192 (1998)
6. Calabi, E., Olver, P.J., Shakiban, C., Tannenbaum, A., Haker, S.: Differential and numerically invariant signature curves applied to object recognition. Int. J. Comput. Vis. **26**, 107–135 (1998)
7. Cartan, É.: La méthode du repère mobile, la théorie des groupes continus, et les espaces généralisés. Exposés de Géométrie, vol. 5. Hermann, Paris (1935)
8. Cohignac, T., Lopez, C., Morel, J.M.: Integral and local affine invariant parameter and application to shape recognition. In: Pattern Recognition, vol. 1, pp. 9–13, 164–168 (1994)
9. Derksen, H., Kemper, G.: Computational invariant theory. In: Invariant Theory and Algebraic Transformation Groups, I. Encyclopedia of Mathematical Sciences, vol. 130. Springer, Berlin (2002)
10. Faugeras, O.: Cartan's moving frame method and its application to the geometry and evolution of curves in the Euclidean, affine and projective planes. In: Mundy, J.L., Zisserman, A., Forsyth, D. (eds.) Application of Invariance in Computer Vision. Lecture Notes in Computer Science, vol. 825, pp. 11–46. Springer, Berlin (1994)
11. Fels, M., Olver, P.J.: Moving coframes. II. Regularization and theoretical foundations. Acta Appl. Math. **55**, 127–208 (1999)
12. Feng, S., Aouada, D., Krim, H., Kogan, I.: 3D mixed invariant and its application on object classification. In: Proceedings of ICASSP, p. 11p, Honolulu, HI (2007)
13. Feng, S., Kogan, I., Krim, H.: Integral invariants for 3D curves: an Inductive Construction. In: Proceedings of IS&T/SPIE Joint Symposium, p. 11p, San Jose, CA (2007)
14. Feng, S., Krim, H., Kogan, I.A.: 3D Face recognition using Euclidean integral invariants signature. In: Proceedings of the 14th Workshop on Signal Processing, pp. 156–160, Honolulu, HI (2007)
15. Green, M.L.: The moving frame, differential invariants and rigidity theorems for curves in homogeneous spaces. Duke Math. J. **45**, 735–779 (1978)
16. Griffiths, P.A.: On Cartan's method of Lie groups as applied to uniqueness and existence questions in differential geometry. Duke Math. J. **41**, 775–814 (1974)
17. Hann, C., Hickman, M.: Projective curvature and integral invariants. Acta Appl. Math. **74**, 177–193 (2002)
18. Hubert, E., Kogan, I.A.: Rational invariants of an algebraic group action: Construction and rewriting. J. Symb. Comput. **42**, 203–217 (2007)
19. Hubert, E., Kogan, I.A.: Smooth and algebraic invariants of a group action: local and global construction. Found. Comput. Math. J. **7**(4), 345–383 (2007)
20. Image database, http://shape.cs.princeton.edu/benchmark/ (2005)
21. Jensen, D.: Higher Order Contact of Submanifolds of Homogeneous Spaces. Lecture Notes in Mathematics, vol. 610. Springer, Berlin (1977)
22. Kogan, I.A.: Two algorithms for a moving frame construction. Can. J. Math. **55**, 266–291 (2003)
23. Lin, W.Y., Boston, N., Hu, Y.H.: Summation invariant and its application to shape recognition. In: Proc. of ICASSP (2005)
24. Manay, S., Cremers, D., Hong, B., Yezzi, A., Soatto, S.: Shape matching via integral invariants. IEEE Trans. Pattern Anal. Mach. Intell. **28**(10), 1602–1618 (2006)
25. Manay, S., Yezzi, A., Hong, B., Soatto, S.: Integral invariant signatures. In: Proc. of the ECCV (2004)
26. Mundy, J.L., Zisserman, A. (eds.): Geometric Invariance in Computer Vision. Artificial Intelligence. MIT Press, Cambridge (1992)
27. Mundy, J.L., Zisserman, A., Forsyth, D. (eds.): Application of Invariance in Computer Vision. Lecture Notes in Computer Science. Springer, Berlin (1992)
28. Mio, W., Bowers, J.C., Hurdal, M.K., Liu, X. (eds.): Modeling brain anatomy with 3D arrangements of curves. In: Proceedings of ICCV, pp. 1–8 (2007)
29. Olver, P.J.: Joint invariant signatures. Found. Comput. Math. **1**, 3–67 (2001)
30. Olver, P.J., Sapiro, G., Tannenbaum, A.: Invariant geometric evolutions of surfaces and volumetric smoothing. SIAM J. Appl. Math. **57**, 176–194 (1997)

31. Sato, J., Cipolla, R.: Affine integral invariants for extracting symmetry axes. Image Vis. Comput. **15**, 627–635 (1997)
32. Sener, S., Unel, M.: A new affine invariant curve normalization technique using independent component analysis. In: Proceedings of ICPR, p. 48, Hong Kong (2006)
33. Sturmfels, B.: Algorithms in Invariant Theory. Springer, Berlin (1993)
34. Taubin, G., Cooper, D.: Object recognition based on moment (or algebraic) invariants. In: Mundy, J.L., Zisserman, A. (eds.) Geometric Invariance in Computer Vision, pp. 375–397. MIT Press, Cambridge (1992)
35. Tieng, Q.M., Boles, W.W.: Wavelet-based affine invariant representation: a tool for recognizing planar objects in 3D space. IEEE Trans. Pattern Anal. Mach. Intell. **19**(8), 846–857 (1997)
36. Tresse, A.R.: Sur les invariants defférentiels des group continus de transformations. Acta Math. **18**, 1–88 (1894)
37. Van Gool, L., Moons, T., Pauwels, E., Oosterlinck, A.: Semi-differential invariants. In: Mundy, J.L., Zisserman, A. (eds.) Geometric Invariance in Computer Vision, pp. 157–192. MIT Press, Cambridge (1992)
38. Van Gool, L., Brill, M., Barrett, E., Moons, T., Pauwels, E.: Semi-differential invariants for non-planar curves. In: Mundy, J.L., Zisserman, A. (eds.) Geometric Invariance in Computer Vision, pp. 157–192. MIT Press, Cambridge (1992)
39. Wang, Y., Teoh, E.K.: 2D affine-invariant contour matching using B-spline model. IEEE Trans. Pattern Anal. Mach. Intell. **29**(10), 1853–1858 (2007)
40. Weiss, I.: Geometric invariants and object recognition. Acta Appl. Math. **10**, 207–231 (1993)
41. Xu, D., Li, H.: 3-D affine moment invariants generated by geometric primitives. In: Proceedings of ICPR, pp. 544–547 (2006)